ICES REPORT 18-17

August 2018

Direct Serendipity and Mixed Finite Elements on Convex Quadrilaterals

by

Todd Arbogast and Zhen Tao

The Institute for Computational Engineering and Sciences
The University of Texas at Austin
Austin, Texas 78712

Reference: Todd Arbogast and Zhen Tao, "Direct Serendipity and Mixed Finite Elements on Convex Quadrilaterals," ICES REPORT 18-17, The Institute for Computational Engineering and Sciences, The University of Texas at Austin, August 2018.

DIRECT SERENDIPITY AND MIXED FINITE ELEMENTS ON CONVEX QUADRILATERALS*

TODD ARBOGAST† AND ZHEN TAO‡

Abstract. The classical serendipity and mixed finite element spaces suffer from poor approximation on nondegenerate, convex quadrilaterals. In this paper, we develop *direct serendipity* and *direct mixed* finite element spaces, which achieve optimal approximation properties and have minimal local dimension. The set of local shape functions for either the serendipity or mixed elements contains the full set of scalar or vector polynomials of degree r, respectively, defined directly on each element (i.e., not mapped from a reference element). Because there are not enough degrees of freedom for global H^1 or $H(\mathrm{div})$ conformity, exactly two supplemental shape functions must be added to each element. The specific choice of supplemental functions gives rise to different families of direct elements. These new spaces are related through a de Rham complex. For index $r \geq 1$, the new families of serendipity spaces $\mathcal{DS}_{r+1}$ are the precursors under the curl operator of our direct mixed finite element spaces $\mathbf{V}_r$, which can be constructed to have full or reduced $H(\mathrm{div})$ approximation properties. One choice of direct serendipity supplements gives the precursor of the recently introduced Arbogast-Correa spaces [SIAM J. Numer. Anal., 54 (2016), pp. 3332–3356]. Other *fully* direct serendipity supplements can be defined without the use of mappings from reference elements, and these give rise in turn to *fully* direct mixed spaces. Numerical results are presented to illustrate the properties of the new spaces.

Key words. serendipity, mixed, finite elements, convex quadrilaterals, optimal approximation, finite element exterior calculus

AMS subject classifications. 65N30, 65N12, 65D05

1. Introduction.

On a rectangle $\hat{E}$, serendipity finite elements $\mathcal{S}_r(\hat{E})$ [39, 20, 17] and Brezzi-Douglas-Marini mixed finite elements $\mathrm{BDM}_r(\hat{E})$ [18] appear in the periodic table of the finite elements as given by Arnold and Logg [11] (where they are denoted $\mathcal{S}_r\Lambda^0$ and $\mathcal{S}_r\Lambda^1$, respectively). They should be studied together, since they are related by a de Rham complex [9, 3, 10]

$$\mathbb{R} \hookrightarrow \mathcal{S}_{r+1}(\hat{E}) \xrightarrow{\mathrm{curl}} \mathrm{BDM}_r(\hat{E}) \xrightarrow{\mathrm{div}} \mathbb{P}_{r-1}(\hat{E}) \longrightarrow 0, \tag{1.1}$$

which implies that $\mathrm{BDM}_r(\hat{E}) = \mathrm{curl}\,\mathcal{S}_{r+1}(\hat{E}) \oplus \mathbf{x}\mathbb{P}_{r-1}(\hat{E})$, where $\mathbb{P}_s(\hat{E})$ are polynomials of degree s. Over a rectangular mesh, the serendipity elements merge into H^1 conforming spaces of scalar functions, and the BDM elements merge into $H(\mathrm{div}) = \left\{\mathbf{v} \in (L^2)^2 : \nabla\cdot\mathbf{v} \in L^2\right\}$ conforming spaces of vector functions. In this paper, we define new (we call them *direct*) serendipity and mixed finite elements on a general nondegenerate, convex quadrilateral E. These new elements generalize the complex (1.1), and they maintain optimal order approximation properties while possessing minimal local dimension.

The serendipity finite elements on rectangles $\mathcal{S}_r(\hat{E})$, especially the 8-node biquadratic ($r = 1$) and the 12-node bicubic ($r = 2$) ones, have been well studied for many years. They appear in almost any introductory reference on finite elements, e.g., [39, 20, 17], and they are provided by software packages both in academia [23] and industry [29]. Compared with the full tensor product Lagrange finite elements

*This work was supported by the U.S. National Science Foundation under grants DMS-1418752 and DMS-1720349.

†University of Texas at Austin; Department of Mathematics, C1200; Austin, TX 78712-1202 and Institute for Computational Engineering and Sciences, C0200; Austin, TX 78712-1229 (arbogast@ices.utexas.edu)

‡University of Texas at Austin; Institute for Computational Engineering and Sciences, C0200; Austin, TX 78712–1229 (taozhen.cn@gmail.com)

$\mathbb{P}_{r,r}(\hat{E})$, serendipity finite elements use fewer degrees of freedom, and they are usually more efficient. It was not until recently, however, that a general definition of the serendipity finite element spaces of arbitrary order on rectangles in any space dimension was given by Arnold and Awanou [4, 5] (see also [26]).

The serendipity finite element spaces work very well on computational meshes of rectangular elements, but it is well known that their performance is degraded on quadrilaterals when the space is mapped from a rectangle, when $r \geq 2$. This is not the case for tensor product Lagrange finite elements [32, 30, 6]. To be more precise, mapped serendipity elements of index r do not approximate to optimal order $r+1$ on E, but the image of the full space of tensor product polynomials $\mathbb{P}_{r,r}(\hat{E})$ maintains accuracy on E. We note that Rand, Gillette, and Bajaj [34] recently introduced a new family of Serendipity finite elements based on generalized barycentric coordinates of index $r = 2$ that is accurate to order three on any convex, planar polygon. A generalization to any order of approximation was given by Floater and Lai [25], but on quadrilaterals, they require $\dim \mathbb{P}_r + r$ shape functions, which is more than the minimal required when $r > 2$.

There are many families of mixed finite elements on rectangles, beginning with those of Raviart and Thomas [35] and generalized by Nédélec [33]. These and the BDM_r finite elements are extended to quadrilaterals using the Piola transform [41, 35]. For most spaces, this creates a consistency error and consequent loss of approximation of the divergence [41, 19, 7, 14, 1].

The construction of mixed finite elements on quadrilaterals that maintain optimal order accuracy is considered in many papers. Most address only low order cases (see, e.g., [37, 36, 15, 13, 22, 31]). The exceptions we are aware of are the families of finite elements of Arnold, Boffi, and Falk (ABF_r(E)) [7], Siqueira, Devloo, and Gomes [38], and Arbogast and Correa ($\mathrm{AC}_r(E)$ and $\mathrm{AC}_r^{\mathrm{red}}(E)$) [1]. The ABF elements are defined for rectangles and extended to quadrilaterals in the usual way (i.e., by mapping via the Piola transformation). They rectify the problem of poor divergence approximation by including more degrees of freedom in the space, so that approximation properties are maintained after Piola mapping. The spaces of [38] also involve the Piola map, but in a unique way. They also add shape functions to their space to obtain accuracy. The AC elements use a different strategy. These elements are defined by using vector polynomials directly on the element (i.e., without being mapped) and supplemented by two vector shape functions defined on a reference square and mapped via Piola. The AC spaces have minimal local dimension.

In this paper, we introduce new families of *direct* serendipity and mixed finite elements that have optimal approximation properties and maintain minimal local dimension. They are *direct* in the sense that the shape functions contain a full set of polynomials defined directly on the element, as in the AC spaces. Because there are not enough degrees of freedom to achieve H^1 or $H(\mathrm{div})$ conformity over meshes of quadrilaterals, two supplemental functions need to be added to each element, as is done for the AC spaces.

The families of direct serendipity elements have the same number of degrees of freedom as the corresponding classical serendipity element, and they take the form

$$\mathcal{DS}_r(E) = \mathbb{P}_r(E) \oplus \mathbb{S}_r^{\mathcal{DS}}(E), \quad r \geq 2. \tag{1.2}$$

Each family is defined by the choice of the two supplemental functions spanning $\mathbb{S}_r^{\mathcal{DS}}(E)$. We give a very general and explicit construction for these supplements. They can be defined directly on E, or they can be defined on $\hat{E}$ and mapped to E.

There are two classes of families of direct mixed elements, which correspond to full and reduced $H(\mathrm{div})$-approximation. For index r, a vector function is approximated to order $r+1$ accuracy, but the divergence of the vector is approximated to order r or $r-1$ for full and reduced $H(\mathrm{div})$-approximation, respectively. Each class of direct mixed elements has the same optimal number of degrees of freedom as the AC elements of that class. They take a form similar to (1.2), which is

$$\mathbf{V}_r^{\mathrm{red}}(E) = \mathbb{P}_r^2(E) \oplus \mathbb{S}_r^{\mathbf{V}}(E), \quad \mathbf{V}_r^{\mathrm{full}}(E) = \mathbf{V}_r^{\mathrm{red}}(E) \oplus \mathbf{x}\tilde{\mathbb{P}}_r(E), \quad r \geq 1, \tag{1.3}$$

where $\tilde{\mathbb{P}}_r$ are homogeneous polynomials of degree r. Again, each family is defined by the choice of the two supplemental functions spanning $\mathbb{S}_r^{\mathbf{V}}(E)$.

The serendipity and mixed families are related by de Rham theory:

$$\operatorname{curl} \mathbb{S}_{r+1}^{\mathcal{DS}}(E) = \mathbb{S}_r^{\mathbf{V}}(E). \tag{1.4}$$

We define one family of direct serendipity elements that is the precursor of the full and reduced AC spaces. We also define many *fully* direct serendipity elements that use no mappings to define $\mathbb{S}_r^{\mathcal{DS}}(E)$, which in turn generate new full and reduced *fully* direct mixed spaces that use no mappings whatsoever. Moreover, a second de Rham complex involving the gradient and curl operators provides new $H(\mathrm{curl}) = \left\{\mathbf{v} \in (L^2)^2 : \operatorname{curl} \mathbf{v} \in L^2\right\}$ elements as well.

We set some basic notation in the next section. For any index $r \geq 2$, we construct new families of direct serendipity elements in Sections 3–4 for which the supplements either do not or do involve mappings, respectively. Through the de Rham theory, these lead to the AC and new direct mixed elements in Section 5. We discuss the stability and convergence properties of the new elements in Section 6, and give some numerical results illustrating their performance in Section 7. A summary of our results and conclusions, as well as $H(\mathrm{curl})$ elements, are given in the final section.

2. Some notation. Let $\mathbb{P}_r(\omega)$ denote the space of polynomials of degree up to r on $\omega \subset \mathbb{R}^d$, where $d = 0$ (a point), 1, or 2. Recall that

$$\dim \mathbb{P}_r(\mathbb{R}^d) = \binom{r+d}{d} = \frac{(r+d)!}{r!\,d!}. \tag{2.1}$$

Let $\tilde{\mathbb{P}}_r(\omega)$ denote the space of homogeneous polynomials of degree r on ω. Then

$$\dim \tilde{\mathbb{P}}_r(\mathbb{R}^d) = \binom{r+d-1}{d-1} = \frac{(r+d-1)!}{r!\,(d-1)!}. \tag{2.2}$$

Let the element $E \subset \mathbb{R}^2$ be a closed, nondegenerate, convex quadrilateral. By nondegenerate, we mean that E does not degenerate to a triangle, line segment, or point. Let the reference element $\hat{E}$ be $[-1,1]^2$. Define the bilinear and bijective map $\mathbf{F}_E : \hat{E} \to E$ that maps the vertices of $\hat{E}$ to those of E. We identify "vertical" and "horizontal" pairs of opposite edges and number them consecutively as shown in Figure 2.1. Let ν_i denote the unit outer normal to edge i (denoted e_i), $i = 1, 2, 3, 4$, and identify the vertices as $\mathbf{x}_{v,13} = e_1 \cap e_3$, $\mathbf{x}_{v,14} = e_1 \cap e_4$, $\mathbf{x}_{v,23} = e_2 \cap e_3$, and $\mathbf{x}_{v,24} = e_2 \cap e_4$.

We define the linear polynomial $\lambda_i(\mathbf{x})$ giving the distance of $\mathbf{x} \in \mathbb{R}^2$ to edge e_i in the normal direction as

$$\lambda_i(\mathbf{x}) = -(\mathbf{x} - \mathbf{x}_i) \cdot \nu_i, \quad i = 1, 2, 3, 4, \tag{2.3}$$

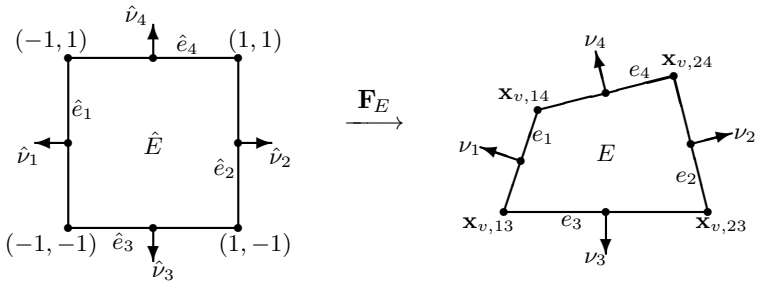

FIG. 2.1. *A reference element $\hat{E} = [-1,1]^2$ and quadrilateral E, with edges $\hat{e}_i$ and e_i, outer unit normals $\hat{\nu}_i$ and ν_i, and vertices $(-1,-1)$ and $\mathbf{x}_{v,13}$, etc., respectively.*

where $\mathbf{x}_i \in e_i$ is any point on the edge. If $\mathbf{x}$ is in the interior of E, these functions are strictly positive, and each vanishes on the edge which defines it.

We denote by F_E^0 the map taking a function $\hat{\phi}$ defined on $\hat{E}$ to a function ϕ defined on E by the rule

$$\phi(\mathbf{x}) = F_E^0(\hat{\phi})(\mathbf{x}) = \hat{\phi}(\hat{\mathbf{x}}), \tag{2.4}$$

where $\mathbf{x} = \mathbf{F}_E(\hat{\mathbf{x}})$. We denote by $\mathbf{F}_E^1$ the Piola map taking a vector function $\hat{\boldsymbol{\psi}}$ defined on $\hat{E}$ to a vector function $\boldsymbol{\psi}$ defined on E by the rule

$$\boldsymbol{\psi}(\mathbf{x}) = \frac{1}{J_E} DF_E(\hat{\mathbf{x}})\, \hat{\boldsymbol{\psi}}(\hat{\mathbf{x}}), \tag{2.5}$$

where $DF_E(\hat{\mathbf{x}})$ is the Jacobian matrix of $\mathbf{F}_E$ and J_E is its absolute determinant.

Recall Ciarlet's definition [20] of a finite element.

DEFINITION 2.1 (Ciarlet 1978). *Let*

1. *$E \subset \mathbb{R}^d$ be a bounded closed set with nonempty interior and a Lipschitz continuous boundary,*
2. *$\mathcal{P}$ be a finite-dimensional space of functions on E, and*
3. *$\mathcal{N} = \{N_1, N_2, \ldots, N_k\}$ be a basis for $\mathcal{P}'$.*

Then $(E, \mathcal{P}, \mathcal{N})$ is called a finite element.

Our task is to define the *shape functions* $\mathcal{P}$ and the *degrees of freedom* (DoFs) $\mathcal{N}$. The DoFs give a basis for $\mathcal{P}'$ provided that we have unisolvence of the shape functions (i.e., for $\phi \in \mathcal{P}$, $N_j(\phi) = 0$ for all j implies that $\phi = 0$). To achieve optimal approximation properties, we will require that $\mathcal{P} \supset \mathbb{P}_r(E)$ for each index r. That is, the polynomials will be directly included within the function space, and hence we call our new finite elements *direct serendipity* and *direct mixed* elements.

Let $\Omega \subset \mathbb{R}^2$ be a polygonal domain, and let $\mathcal{T}_h$ be a conforming finite element partition or mesh of Ω into nondegenerate, convex quadrilaterals of maximal diameter $h > 0$. To obtain approximation properties globally, we need to assume that the mesh is uniformly shape regular [27, pp. 104–105], which means the following. For any $E \in \mathcal{T}_h$, denote by T_i, $i = 1, 2, 3, 4$, the subtriangle of E with vertices being three of the four vertices of E. Define the parameters

$$h_E = \text{diameter of } E, \tag{2.6}$$

$$\rho_E = 2 \min_{1 \le i \le 4} \{\text{diameter of largest circle inscribed in } T_i\}. \tag{2.7}$$

Uniform shape regularity of the meshes means that there exists $\sigma_* > 0$ such that the ratio $\rho_E/h_E \geq \sigma_* > 0$ for all $E \in \mathcal{T}_h$, where σ_* is independent of $\mathcal{T}_h$.

The DoFs must be defined so that the shape functions on adjoining elements merge together. For serendipity spaces, we want the global space to reside in $H^1(\Omega)$, so the elements must merge continuously across each edge e. For mixed spaces, the vector variable must lie in $H(\mathrm{div};\Omega)$, which means that the normal components (fluxes) of the vectors on an edge e in adjacent elements must be continuous.

3. Fully direct serendipity elements in two space dimensions. It is shown in [6] that when $d = 2$, the convergence of the linear serendipity finite element space ($r = 1$) does not degenerate on quadrilaterals. The parametric serendipity element $\mathcal{S}_1(E)$ is the tensor product space of bilinear functions $\mathbb{P}_{1,1}(\hat{E})$ on $\hat{E}$ mapped to E by F_E^0, and, in fact,

$$\begin{aligned}\mathcal{S}_1(E) &= \mathrm{span}\{F_E^0(1), F_E^0(\hat{x}), F_E^0(\hat{y}), F_E^0(\hat{x}\hat{y})\} \\ &= \mathrm{span}\{1, x, y, F_E^0(\hat{x}\hat{y})\} = \mathbb{P}_1(E) \oplus \mathrm{span}\{F_E^0(\hat{x}\hat{y})\}\end{aligned} \tag{3.1}$$

has the form of a direct serendipity space. Therefore, we only develop our new direct serendipity finite elements $\mathcal{DS}_r(E)$ for indices $r \geq 2$.

Our dual objectives are that $\mathbb{P}_r(E) \subset \mathcal{DS}_r(E)$ and that shape functions on adjoining elements merge continuously, i.e., so the space over Ω satisfies $\mathcal{DS}_r(\Omega) \subset H^1(\Omega)$. These objectives require us to consider the lower dimensional geometric objects within E (as in [4]). The minimal number of DoFs associated to each lower dimensional object must correspond to the dimension of the polynomials that restrict to that object. These numbers are given in Table 3.1. A quadrilateral has 4 vertices, 4 edges, and one cell of dimension 0, 1, and 2, respectively. Each vertex requires $\dim \mathbb{P}(\mathbb{R}^0) = 1$ DoF, each edge requires $\dim \mathbb{P}_{r-2}(\mathbb{R}) = r - 1$ DoFs (not counting the vertices), and each cell requires $\dim \mathbb{P}_{r-4}(\mathbb{R}^2) = \binom{r-2}{2}$ DoFs (not counting the edges and vertices). The total number of DoFs is then D_r, where

$$D_r = 4 + 4(r-1) + \frac{1}{2}(r-2)(r-3) = \frac{1}{2}(r+2)(r+1) + 2 = \dim \mathbb{P}_r(E) + 2,$$

and so to define $\mathcal{DS}_r(E)$, we will supplement $\mathbb{P}_r(E) \subset \mathcal{DS}_r(E)$ with the span of two functions. We have many choices for the supplemental functions, the span of which is denoted $\mathbb{S}_r^{\mathcal{DS}}(E)$. Each choice gives rise to a distinct family of direct serendipity elements of index $r \geq 2$; that is, the shape functions ($\mathcal{P}$ in Definition 2.1) are

$$\mathcal{DS}_r(E) = \mathbb{P}_r(E) \oplus \mathbb{S}_r^{\mathcal{DS}}(E). \tag{3.2}$$

In this section, we develop supplemental spaces that are unmapped (i.e., these new serendipity spaces are fully direct—even the supplements are defined directly on E).

We define the DoFs ($\mathcal{N}$ in Definition 2.1) as a set of nodal functionals N_j defined at a nodal point $\mathbf{x}_{n,j}$, i.e.,

$$\mathcal{N} = \{N_j : N_j(\phi) = \phi(\mathbf{x}_{n,j}) \text{ for all } \phi(\mathbf{x}),\ j = 1, 2, \ldots, D_r\}. \tag{3.3}$$

As depicted in Figure 3.1, for vertex DoFs, the nodal points are exactly the vertices $\mathbf{x}_{v,13}$, $\mathbf{x}_{v,14}$, $\mathbf{x}_{v,23}$, and $\mathbf{x}_{v,24}$ of E. For edge DoFs, the nodal points plus vertices are equally distributed on each edge. There are $r - 1$ nodal points on the interior of each egde, which can be denoted $\mathbf{x}_{e_i,j}$, $j = 1, \ldots, r-1$ for nodal points that lie on edge e_i, $i = 1, 2, 3, 4$. The interior cell DoFs can be set, for example, on points of a triangle T strictly inside E, where the set of nodal points is the same as the nodes of the Lagrange element of order $r - 4$ on the triangle T.

TABLE 3.1
Geometric decomposition and degrees of freedom (DoFs) associated to each geometric object of a quadrilateral for a serendipity element of index $r \geq 2$.

Dimension	Object Name	Object Count	DoFs per Object	Total DoFs
0	vertex	4	1	4
1	edge	4	$r-1$	$4(r-1)$
2	cell	1	$\frac{1}{2}(r-2)(r-3)$	$\frac{1}{2}(r-2)(r-3)$

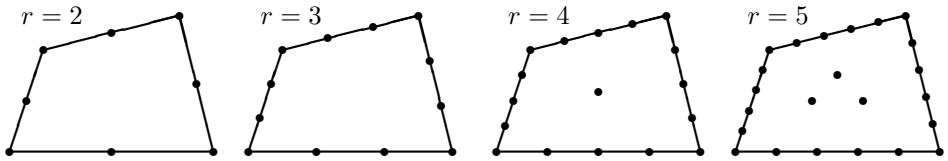

FIG. 3.1. *The nodal points for the DoFs of the direct serendipity finite element for small r.*

3.1. Vertices. For the vertices, $r \geq 2$, so we can define the shape functions

$$\begin{aligned} \phi_{v,13}(\mathbf{x}) &= \lambda_2(\mathbf{x})\lambda_4(\mathbf{x}), \quad \phi_{v,14}(\mathbf{x}) = \lambda_2(\mathbf{x})\lambda_3(\mathbf{x}), \\ \phi_{v,23}(\mathbf{x}) &= \lambda_1(\mathbf{x})\lambda_4(\mathbf{x}), \quad \phi_{v,24}(\mathbf{x}) = \lambda_1(\mathbf{x})\lambda_3(\mathbf{x}). \end{aligned} \tag{3.4}$$

These four functions are clearly linearly independent and unisolvent with respect to the vertex DoFs. All other shape functions will be defined so as to vanish at the vertices, so these four will be independent of the rest.

3.2. Interior cell. For the entire cell E, we need interior shape functions only when $r \geq 4$ (recall Table 3.1). We let the shape functions be defined by

$$\big\{\phi_{E,j}(\mathbf{x}) : j = 1, \dots, \tfrac{1}{2}(r-2)(r-3)\big\} = \lambda_1\lambda_2\lambda_3\lambda_4\mathbb{P}_{r-4}. \tag{3.5}$$

These shape functions are linearly independent and vanish if the cell DoFs vanish. Moreover, these functions vanish on all four edges. Therefore, if unisolvent shape functions can be defined for the edge DoFs, then the set of all our shape functions will be unisolvent for the entire set of DoFs.

3.3. Edges. We define distinct families of fully direct serendipity elements depending on the choice of the two supplemental functions used. These will be defined by a choice of four functions, which are oriented "horizontally" or "vertically," in the sense that their zero sets are horizontal or vertical (as oriented by the bilinear map $\mathbf{F}_E$, see Figure 2.1). Two of the functions are linear polynomials, denoted λ_H and λ_V. The other two functions should be bounded, and they are denoted R_V and R_H. The supplemental space is then defined as

$$\mathbb{S}_r^{\mathcal{DS}}(E) = \operatorname{span}\{\lambda_3\lambda_4\lambda_H^{r-2}R_V, \lambda_1\lambda_2\lambda_V^{r-2}R_H\}. \tag{3.6}$$

The choice of the linear function λ_H is based on the edges e_1 and e_2. As shown in Figure 3.2, let $\mathcal{L}_1$ and $\mathcal{L}_2$ be the infinite lines containing the edges e_1 and e_2, respectively. When e_1 and e_2 are parallel, the only requirement for the choice of λ_H is that its zero line intersects both $\mathcal{L}_1$ and $\mathcal{L}_2$. When e_1 and e_2 are not parallel, $\mathcal{L}_1$ and $\mathcal{L}_2$ intersect in a point $\mathbf{x}_{12}$. Then the only requirements for the choice of λ_H is that $\lambda_H(\mathbf{x}_{12}) \neq 0$ and that its zero line intersects both $\mathcal{L}_1$ and $\mathcal{L}_2$ on the half-lines

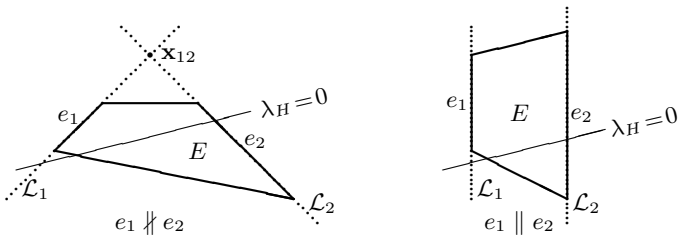

FIG. 3.2. *Illustration of the zero lines of λ_H and the point $\mathbf{x}_{12}$, if it exists.*

emanating from $\mathbf{x}_{12}$ and either containing e_1 and e_2, respectively, or not containing e_1 and e_2, respectively (i.e., the zero line of λ_H intersects the lines containing e_1 and e_2 either above or below $\mathbf{x}_{12}$). To be more precise in the case when e_1 and e_2 are not parallel, we can expand $\lambda_H \in \mathbb{P}_1(\mathbb{R}^2)$ in the basis defined by $\{1, \lambda_1, \lambda_2\}$, so there are constants α_H, β_H, and γ_H such that

$$\lambda_H(\mathbf{x}) = \alpha_H \lambda_1(\mathbf{x}) + \beta_H \lambda_2(\mathbf{x}) + \gamma_H = -(\mathbf{x} - \mathbf{x}_H) \cdot (\alpha_H \nu_1 + \beta_H \nu_2), \quad e_1 \nparallel e_2, \tag{3.7}$$

where $\mathbf{x}_H$ is any point on the zero line. The requirements are that α_H, β_H, and γ_H are nonzero and that α_H and β_H have the same sign. Without loss of generality, we may assume that α_H and β_H are positive. In a similar way, λ_V is chosen to intersect the lines extending e_3 and e_4, and when they are not parallel, either strictly to the left or right of the intersection point $\mathbf{x}_{34}$. When e_3 and e_4 are not parallel,

$$\lambda_V(\mathbf{x}) = \alpha_V \lambda_1(\mathbf{x}) + \beta_V \lambda_2(\mathbf{x}) + \gamma_V See = -(\mathbf{x} - \mathbf{x}_V) \cdot (\alpha_V \nu_1 + \beta_V \nu_2), \quad e_3 \nparallel e_4, \tag{3.8}$$

where $\mathbf{x}_V$ is any point on the zero line, $\alpha_V > 0$, $\beta_V > 0$, and $\gamma_V \neq 0$. We remark that a simple choice is to take

$$\lambda_H^{\text{simple}} = \lambda_3 - \lambda_4 \quad \text{and} \quad \lambda_V^{\text{simple}} = \lambda_1 - \lambda_2. \tag{3.9}$$

The functions R_V and R_H are defined to satisfy the properties

$$R_V(\mathbf{x})|_{e_1} = -\eta_V \quad \text{and} \quad R_V(\mathbf{x})|_{e_2} = \xi_V, \tag{3.10}$$

$$R_H(\mathbf{x})|_{e_3} = -\eta_H \quad \text{and} \quad R_H(\mathbf{x})|_{e_4} = \xi_H, \tag{3.11}$$

for some positive constants η_V, ξ_V, η_H, and ξ_H. For example, one choice is to let

$$R_V^{\text{simple}}(\mathbf{x}) = \frac{\lambda_1(\mathbf{x}) - \lambda_2(\mathbf{x})}{\xi_V^{-1}\lambda_1(\mathbf{x}) + \eta_V^{-1}\lambda_2(\mathbf{x})}, \tag{3.12}$$

$$R_H^{\text{simple}}(\mathbf{x}) = \frac{\lambda_3(\mathbf{x}) - \lambda_4(\mathbf{x})}{\xi_H^{-1}\lambda_3(\mathbf{x}) + \eta_H^{-1}\lambda_4(\mathbf{x})} \tag{3.13}$$

(note that the denominators do not vanish on E).

We now define the shape functions associated with the edge DoFs. Let

$$\lambda_{12} = \begin{cases} \alpha_H \xi_V \lambda_1 - \beta_H \eta_V \lambda_2, & e_1 \nparallel e_2, \\ \xi_V \lambda_1 - \eta_V \lambda_2, & e_1 \parallel e_2, \end{cases} \tag{3.14}$$

$$\lambda_{34} = \begin{cases} \alpha_V \xi_H \lambda_3 - \beta_V \eta_H \lambda_4, & e_3 \nparallel e_4, \\ \xi_H \lambda_3 - \eta_H \lambda_4, & e_3 \parallel e_4, \end{cases} \tag{3.15}$$

which also have horizontal and vertical zero sets, respectively. There are $2(r-1)$ shape functions associated to the edges e_1 and e_2, and they are

$$\phi_{H,j}(\mathbf{x}) = \lambda_3(\mathbf{x})\lambda_4(\mathbf{x})\lambda_H^j(\mathbf{x}), \qquad j = 0, 1, \dots, r-2, \tag{3.16}$$

$$\phi_{H,r-1+j}(\mathbf{x}) = \lambda_3(\mathbf{x})\lambda_4(\mathbf{x})\lambda_{13}(\mathbf{x})\lambda_H^j(\mathbf{x}), \qquad j = 0, 1, \dots, r-3, \tag{3.17}$$

$$\phi_{H,2r-3}(\mathbf{x}) = \lambda_3(\mathbf{x})\lambda_4(\mathbf{x})R_V(\mathbf{x})\lambda_H^{r-2}(\mathbf{x}). \tag{3.18}$$

In a similar way, we define shape functions associated with edges e_3 and e_4 to be

$$\phi_{V,j}(\mathbf{x}) = \lambda_1(\mathbf{x})\lambda_2(\mathbf{x})\lambda_V^j(\mathbf{x}), \qquad j = 0, 1, \dots, r-2, \tag{3.19}$$

$$\phi_{V,r-1+j}(\mathbf{x}) = \lambda_1(\mathbf{x})\lambda_2(\mathbf{x})\lambda_{24}(\mathbf{x})\lambda_V^j(\mathbf{x}), \qquad j = 0, 1, \dots, r-3, \tag{3.20}$$

$$\phi_{V,2r-3}(\mathbf{x}) = \lambda_1(\mathbf{x})\lambda_2(\mathbf{x})R_H(\mathbf{x})\lambda_V^{r-2}(\mathbf{x}). \tag{3.21}$$

The edge shape functions are regular polynomials of degree r except the last two functions in each direction, which may be rational functions, for example. However, all shape functions restrict to polynomials of degree r on the edges.

3.4. Unisolvence. The space of shape functions is

$$\begin{aligned} \mathcal{DS}_r(E) = \operatorname{span}\big\{&\phi_{v,13}(\mathbf{x}), \phi_{v,14}(\mathbf{x}), \phi_{v,23}(\mathbf{x}), \phi_{v,24}(\mathbf{x}), \\ &\phi_{H,j}(\mathbf{x}), \phi_{V,j}(\mathbf{x}) \ (j = 0, 1, \dots, 2r-3), \\ &\phi_{E,k}(\mathbf{x}) \ (k = 1, \dots, \tfrac{1}{2}(r-2)(r-3))\big\} \\ \subset\ &\mathbb{P}_r(E) \oplus \mathbb{S}_r^{\mathcal{DS}}(E). \end{aligned} \tag{3.22}$$

In this subsection, we show the unisolvence of the degrees of freedom, which will then show that $\mathcal{DS}_r(E) = \mathbb{P}_r(E) \oplus \mathbb{S}_r^{\mathcal{DS}}(E)$ and complete the requirements of Ciarlet's Definition 2.1 for $\mathcal{DS}_r(E)$ to be a well defined finite element. But first, we require a lemma.

LEMMA 3.1. *Let $k \geq 1$. For any $\eta_V > 0$ and $\xi_V > 0$, there exists a function $\tilde{R}_V$, defined by* (3.23) *and* (3.26)*, with the properties* (3.10) *such that the two function spaces*

$$\begin{aligned} \mathcal{A}_k^1 &= \operatorname{span}\{1, \lambda_H, \dots, \lambda_H^k, \lambda_{12}, \lambda_H\lambda_{12}, \dots, \lambda_H^{k-1}\lambda_{12}, \lambda_H^k\tilde{R}_V\}, \\ \mathcal{A}_k^2 &= \operatorname{span}\big\{\{1, \lambda_H, \dots, \lambda_H^k\} \otimes \{1, \tilde{R}_V\}\big\} \end{aligned}$$

are identical. Moreover, for any $\eta_H > 0$ and $\xi_H > 0$, there exists an $\tilde{R}_H$, defined by (3.27)*, with the properties* (3.11) *such that the two function spaces*

$$\begin{aligned} \mathcal{A}_k^3 &= \operatorname{span}\{1, \lambda_V, \dots, \lambda_V^k, \lambda_{34}, \lambda_V\lambda_{34}, \dots, \lambda_V^{k-1}\lambda_{34}, \lambda_V^k\tilde{R}_H\}, \\ \mathcal{A}_k^4 &= \operatorname{span}\big\{\{1, \lambda_V, \dots, \lambda_V^k\} \otimes \{1, \tilde{R}_H\}\big\} \end{aligned}$$

are identical.

Proof. We show that $\mathcal{A}_k^1 = \mathcal{A}_k^2$. Assume that $e_1 \nparallel e_2$, so that λ_H has the form (3.7) for some $\alpha_H > 0$, $\beta_H > 0$, and $\gamma_H \neq 0$. We define $\tilde{R}_V$ satisfying (3.10) as

$$\tilde{R}_V = \frac{\alpha_H\xi_V\lambda_1 - \beta_H\eta_V\lambda_2}{\alpha_H\lambda_1 + \beta_H\lambda_2} = \frac{\lambda_{12}}{\lambda_H - \gamma_H}, \quad e_1 \nparallel e_2. \tag{3.23}$$

Because α_H and β_H are both positive, the denominator is not zero on E. We compute

$$\tilde{R}_V = \frac{\lambda_{12}}{\lambda_H - \gamma_H} = -\frac{1}{\gamma_H}\lambda_{12} + \frac{1}{\gamma_H}\frac{\lambda_{12}\lambda_H}{\lambda_H - \gamma_H} = -\frac{1}{\gamma_H}\lambda_{12} + \frac{1}{\gamma_H}\lambda_H\tilde{R}_V. \tag{3.24}$$

We show that for any $\ell \geq 0$,

$$\tilde{R}_V = -\sum_{j=1}^{\ell} \frac{1}{\gamma_H^j} \lambda_{12} \lambda_H^{j-1} + \frac{1}{\gamma_H^\ell} \lambda_H^\ell \tilde{R}_V. \tag{3.25}$$

The relation holds trivially for $\ell = 0$, and (3.24) shows the result for $\ell = 1$. Assuming by induction that (3.25) holds for $\ell - 1$, we compute (using (3.24))

$$\begin{aligned}
\tilde{R}_V &= -\sum_{j=1}^{\ell-1} \frac{1}{\gamma_H^j} \lambda_{12} \lambda_H^{j-1} + \frac{1}{\gamma_H^{\ell-1}} \lambda_H^{\ell-1} \tilde{R}_V \\
&= -\sum_{j=1}^{\ell-1} \frac{1}{\gamma_H^j} \lambda_{12} \lambda_H^{j-1} + \frac{1}{\gamma_H^{\ell-1}} \lambda_H^{\ell-1} \left(-\frac{1}{\gamma_H} \lambda_{12} + \frac{1}{\gamma_H} \lambda_H \tilde{R}_V \right) \\
&= -\sum_{j=1}^{\ell} \frac{1}{\gamma_H^j} \lambda_{12} \lambda_H^{j-1} + \frac{1}{\gamma_H^\ell} \lambda_H^\ell \tilde{R}_V,
\end{aligned}$$

and (3.25) holds for all ℓ. Therefore, for any $0 \leq m \leq k$, taking $\ell = k - m$,

$$\lambda_H^m \tilde{R}_V = -\sum_{j=1}^{k-m} \frac{1}{\gamma_H^j} \lambda_{12} \lambda_H^{j-1+m} + \frac{1}{\gamma_H^{k-m}} \lambda_H^k \tilde{R}_V \in \mathcal{A}_k^1,$$

and we conclude that $\mathcal{A}_k^2 \subset \mathcal{A}_k^1$. But clearly $\dim \mathcal{A}_k^2 = 2(k-1)$ and $\dim \mathcal{A}_k^1 \leq 2(k-1)$, and so the spaces are in fact equal.

If $e_1 \parallel e_2$, then $\lambda_{12} = \xi_V \lambda_1 - \eta_V \lambda_2$ and $\lambda_1 + \lambda_2 = \delta_H > 0$ is a constant. We define

$$\tilde{R}_V = \frac{\xi_V \lambda_1 - \eta_V \lambda_2}{\lambda_1 + \lambda_2} = \frac{1}{\delta_H} \lambda_{12}, \quad e_1 \parallel e_2, \tag{3.26}$$

which satisfies (3.10). In this case, it is trivial that $\mathcal{A}_k^2 = \mathcal{A}_k^1$.

By symmetry, $\mathcal{A}_k^3 = \mathcal{A}_k^4$, where now

$$\tilde{R}_H = \begin{cases} \dfrac{\lambda_{34}}{\lambda_V - \gamma_V}, & e_3 \nparallel e_4, \\ \dfrac{1}{\delta_V} \lambda_{34}, & e_3 \parallel e_4, \end{cases} \tag{3.27}$$

where $\lambda_3 + \lambda_4 = \delta_V > 0$ is a constant when $e_3 \parallel e_4$. ∎

THEOREM 3.2. *Let $(E, \mathcal{DS}_r(E), \mathcal{N})$ be the r-th order direct serendipity finite element defined by* (3.22)*, i.e., by* (3.4)*,* (3.5)*, and* (3.16)–(3.21)*) and* (3.3)*. If $\phi \in \mathcal{DS}_r(E)$ and $N_k(\phi) = 0$, for all $k = 1, 2, \ldots, D_r$, then $\phi = 0$. Moreover,*

$$\mathcal{DS}_r(E) = \mathbb{P}_r(E) \oplus \mathbb{S}_r^{\mathcal{DS}}(E), \tag{3.28}$$

where $\mathbb{S}_r^{\mathcal{DS}}(E)$ is defined in (3.6)*.*

Proof. As noted in Subsection 3.2, by construction, the full set of DoFs are unisolvent for $\mathcal{DS}_r(E)$ if the edge DoFs are unisolvent for the edge shape functions $\phi_{H,j}$ and $\phi_{V,j}$. We temporarily replace R_V by $\tilde{R}_V$ defined in (3.23) or (3.26). In that case,

$$\{\phi_{H,j} : j = 0, 1, \ldots, r-2\} = \lambda_3 \lambda_4 \mathcal{A}_{r-2}^1 = \lambda_3 \lambda_4 \mathcal{A}_{r-2}^2,$$

by the lemma, and the representation of the space using $\mathcal{A}^2_{r-2}$ clearly shows that the DoFs on the edges e_1 and e_2 are unisolvent for $\phi_{H,j}$. That is, for an edge shape function $\phi(\mathbf{x})$ with vanishing DoFs, we can use $\mathcal{A}^2_{r-2}$ to expand it as

$$\phi(\mathbf{x}) = \lambda_3(\mathbf{x})\lambda_4(\mathbf{x}) \sum_{\ell=0}^{r-2} \big(a_\ell + R_V(\mathbf{x})\, b_\ell\big)\lambda_H^\ell(\mathbf{x}),$$

for some constants a_ℓ and b_ℓ. On either edge e_1 or e_2 , $\phi(\mathbf{x})$ is a polynomial of degree r, which must vanish due to the vanishing of the DoFs. Therefore, $a_\ell + R_V(\mathbf{x})\, b_\ell$ must vanish on each edge, and we conclude that both $\eta_V a_\ell - \xi_V b_\ell = 0$ and $\eta_V a_\ell + \xi_V b_\ell = 0$, i.e., $a_\ell = b_\ell = 0$, and so $\phi(\mathbf{x}) = 0$. It should be clear that we can return to the original R_V and draw the same conclusion, since the DoFs of any function in the argument are unchanged by this replacement. (Of course, we no longer have that $\mathcal{A}^1_{r-2} = \mathcal{A}^2_{r-2}$, but only that their DoFs agree.) Similarly we conclude unisolvence for $\phi_{V,j}$.

We conclude that $\dim \mathcal{DS}_r(E) = D_r = \dim \mathbb{P}_r(E) + 2$. Since we clearly added only two shape functions not in $\mathbb{P}_r(E)$, the full space of polynomials is contained in $\mathcal{DS}_r(E)$, and $\mathcal{DS}_r(E) = \mathbb{P}_r(E) \oplus \mathbb{S}_r^{\mathcal{DS}}(E)$. ∎

3.5. Implementation as an H^1-Conforming Space. The global direct serendipity finite element space of index $r \geq 2$ over $\mathcal{T}_h$ is

$$\mathcal{DS}_r = \{v_h \in \mathcal{C}^0(\Omega) \,:\, v_h|_E \in \mathcal{DS}_r(E)\ \forall E \in \mathcal{T}_h\} \subset H^1(\Omega). \tag{3.29}$$

To implement H^1-conforming direct serendipity elements on the mesh $\mathcal{T}_h$ over Ω, we need to find a proper basis for the finite element space, i.e., one that is continuous. We observe that the interior cell shape functions, after extension by zero, are in $H^1(\Omega)$ and so cause no difficulty. The vertex and edge shape functions with DoFs on the boundaries of the elements must be merged continuously. The simplest way to do this is to create a local nodal basis on every $E \in \mathcal{T}_h$ for these $4r$ shape functions.

Let ϕ be any one of the shape functions of $\mathcal{DS}_r(E)$ defined above in (3.4), (3.5), and (3.16)–(3.21). To reduce rounding errors in numerical calculations, we scale it so

$$\phi \quad \text{is replaced by} \quad \frac{\phi}{d_E^{n_\phi}},$$

where $d_E = \sqrt{|E|}$ and n_ϕ is the degree of ϕ when it is a polynomial and $n_{\phi_{H,2r-3}} = n_{\phi_{V,2r-3}} = r$.

In general, we can find the local basis $\{\varphi_1, \ldots, \varphi_{4r}\}$ by solving a small local linear system. We order the shape functions with the vertex DoFs first (ϕ_1 to ϕ_4), the horizontal edge DoFs on e_1 and e_2 next (ϕ_5 to ϕ_{2r+2}), and finally the vertical edge DoFs on e_3 and e_4 (ϕ_{2r+3} to ϕ_{4r}). We also order the DoFs similarly. Construct the $4r \times 4r$ matrix $\mathbf{A} = (a_{ij})$ of the DoFs, i.e., $\mathbf{A}_{ij} = N_j(\phi_i)$ for all $i, j \leq 4r$. This matrix has a simple block structure based on the DoFs on the vertices, edges e_1 and e_2, and edges e_3 and e_4, which is

$$\mathbf{A} = \begin{pmatrix} \mathbf{A}_{11} & \mathbf{A}_{12} & \mathbf{A}_{13} \\ \mathbf{0} & \mathbf{A}_{22} & \mathbf{0} \\ \mathbf{0} & \mathbf{0} & \mathbf{A}_{33} \end{pmatrix}, \tag{3.30}$$

where $\mathbf{A}_{11}$ is of size 4×4 and $\mathbf{A}_{22}$ and $\mathbf{A}_{33}$ are of size $2(r-1) \times 2(r-1)$. From Theorem 3.2 (unisolvence), we know that $\mathbf{A}$ is invertible. Let $\mathbf{A}^{-1} = \mathbf{B} = (b_{ij})$ and

define

$$\varphi_i = \sum_{j=1}^{4r} b_{ij}\phi_j \quad \Longrightarrow \quad N_k(\varphi_i) = \sum_{j=1}^{4r} b_{ij}N_k(\phi_j) = \sum_{j=1}^{4r} b_{ij}a_{jk} = \delta_{ik},$$

and we have our nodal basis. Graphical depiction of the basis in special cases can be found in [40, 2]. Visually, there is nothing unusual about these basis functions.

If we take the choice outlined in Lemma 3.1, we can write down the nodal basis explicitly, using the facts that $\mathcal{A}^1_{r-2} = \mathcal{A}^2_{r-2}$ and $\mathcal{A}^3_{r-2} = \mathcal{A}^4_{r-2}$. The edge basis functions become, for $j = 1, \ldots, r-1$,

$$\varphi_{e_1,j}(\mathbf{x}) = \frac{\lambda_3(\mathbf{x})\lambda_4(\mathbf{x})}{\lambda_3(\mathbf{x}_{e_1,j})\lambda_4(\mathbf{x}_{e_1,j})}\frac{\xi_V - \tilde{R}_V(\mathbf{x})}{\xi_V + \eta_V}\prod_{\substack{k=1\\k\neq j}}^{r-1}\frac{\lambda_H(\mathbf{x}) - \lambda_H(\mathbf{x}_{e_1,k})}{\lambda_H(\mathbf{x}_{e_1,j}) - \lambda_H(\mathbf{x}_{e_1,k})}, \tag{3.31}$$

$$\varphi_{e_2,j}(\mathbf{x}) = \frac{\lambda_3(\mathbf{x})\lambda_4(\mathbf{x})}{\lambda_3(\mathbf{x}_{e_2,j})\lambda_4(\mathbf{x}_{e_2,j})}\frac{\tilde{R}_V(\mathbf{x}) + \eta_V}{\xi_V + \eta_V}\prod_{\substack{k=1\\k\neq j}}^{r-1}\frac{\lambda_H(\mathbf{x}) - \lambda_H(\mathbf{x}_{e_2,k})}{\lambda_H(\mathbf{x}_{e_2,j}) - \lambda_H(\mathbf{x}_{e_2,k})}, \tag{3.32}$$

$$\varphi_{e_3,j}(\mathbf{x}) = \frac{\lambda_1(\mathbf{x})\lambda_2(\mathbf{x})}{\lambda_1(\mathbf{x}_{e_3,j})\lambda_2(\mathbf{x}_{e_3,j})}\frac{\xi_H - \tilde{R}_H(\mathbf{x})}{\xi_H + \eta_H}\prod_{\substack{k=1\\k\neq j}}^{r-1}\frac{\lambda_V(\mathbf{x}) - \lambda_V(\mathbf{x}_{e_3,k})}{\lambda_V(\mathbf{x}_{e_3,j}) - \lambda_V(\mathbf{x}_{e_3,k})}, \tag{3.33}$$

$$\varphi_{e_4,j}(\mathbf{x}) = \frac{\lambda_1(\mathbf{x})\lambda_2(\mathbf{x})}{\lambda_1(\mathbf{x}_{e_4,j})\lambda_2(\mathbf{x}_{e_4,j})}\frac{\tilde{R}_H(\mathbf{x}) + \eta_H}{\xi_H + \eta_H}\prod_{\substack{k=1\\k\neq j}}^{r-1}\frac{\lambda_V(\mathbf{x}) - \lambda_V(\mathbf{x}_{e_4,k})}{\lambda_V(\mathbf{x}_{e_4,j}) - \lambda_V(\mathbf{x}_{e_4,k})}. \tag{3.34}$$

The vertex basis function $\varphi_{v,13}(\mathbf{x})$ can be computed by first defining

$$\tilde{\phi}_{v,13}(\mathbf{x}) = \frac{\lambda_2(\mathbf{x})\lambda_4(\mathbf{x})}{\lambda_2(\mathbf{x}_{v,13})\lambda_4(\mathbf{x}_{v,13})},$$

and then defining

$$\varphi_{v,13}(\mathbf{x}) = \tilde{\phi}_{v,13}(\mathbf{x}) - \sum_{k\in\{1,3\}}\sum_{j=1}^{r-1}\tilde{\phi}_{v,13}(\mathbf{x}_{e_k,j})\,\varphi_{e_k,j}(\mathbf{x}). \tag{3.35}$$

The basis functions $\varphi_{v,14}(\mathbf{x})$, $\varphi_{v,23}(\mathbf{x})$, and $\varphi_{v,24}(\mathbf{x})$ can be defined similarly.

4. Serendipity supplements based on mapping from a reference element. The supplemental functions $\mathbb{S}_r^{\mathcal{DS}}(E)$ used in the definition of $\mathcal{DS}_r(E)$ in (3.22) can be defined in terms of the bilinear map $\mathbf{F}_E : \hat{E} \to E$ and F_E^0 discussed in Section 2. For example, since $\hat{E} = [-1, 1]^2$, one can define

$$R_V(\mathbf{x}) = F_E^0(\hat{x}_1) \quad \text{and} \quad R_H(\mathbf{x}) = F_E^0(\hat{x}_2), \tag{4.1}$$

for which $\eta_V = \xi_V = \eta_H = \xi_H = 1$.

We can also use the map to define the entire supplemental functions (3.13) and (3.12) themselves. For example, we can substitute the definitions

$$\phi_{H,2r-3}(\mathbf{x}) = F_E^0\big((1-\hat{x}_2^2)\hat{x}_1\hat{x}_2^{r-2}\big), \tag{4.2}$$

$$\phi_{V,2r-3}(\mathbf{x}) = F_E^0\big((1-\hat{x}_1^2)\hat{x}_2\hat{x}_1^{r-2}\big), \tag{4.3}$$

giving direct serendipity elements with mapped supplements. We must show unisolvence with this substitution. We proceed to show this property for edges e_1 and e_2. The other two edges will then have this property by symmetry.

Easily,

$$\phi_{H,2r-3}(\mathbf{x}) = F_E^0(1-\hat{x}_2^2)\,F_E^0(\hat{x}_1)\left(F_E^0(\hat{x}_2)\right)^{r-2} = F_E^0(1-\hat{x}_2^2)\,R_V\,(\lambda_H^*)^{r-2},$$

where R_V is defined in (4.1) and

$$\lambda_H^* = F_E^0(\hat{x}_2)$$

is a *nonlinear* function. Because $\mathbf{F}_E$ is a bilinear map, on the edges e_1 and e_2, λ_H^* is linear and $F_E^0(1-\hat{x}_2^2)$ is quadratic. However, these may be *different* linear and quadratic functions on each edge.

The function $\lambda_H^* = F_E^0(\hat{x}_2)$ has the zero set being the line joining the center of e_1 to the center of e_2. Let $\mathbf{x}_H$ be any point on this line and ν_H denote a unit normal to the line. Define

$$\lambda_H(\mathbf{x}) = -(\mathbf{x}-\mathbf{x}_H)\cdot\nu_H. \tag{4.4}$$

If e_1 and e_2 are not parallel, then there exist (up to sign, so without loss of generality) $\alpha_H > 0$, $\beta_H > 0$, and $\gamma_H \neq 0$ such that

$$\lambda_H(\mathbf{x}) = \alpha_H\lambda_1(\mathbf{x}) + \beta_H\lambda_2(\mathbf{x}) + \gamma_H.$$

If e_1 and e_2 are parallel, set $\alpha_H = \beta_H = 1$ and $\gamma_H = 0$ to obtain the same representation of λ_H. In either case, we define

$$\lambda_{12} = \alpha_H\lambda_1 - \beta_H\lambda_2 \quad\text{and}\quad \tilde{R}_V = \frac{\alpha_H\lambda_1 - \beta_H\lambda_2}{\alpha_H\lambda_1 + \beta_H\lambda_2}.$$

These functions satisfy the requirements of Lemma 3.1.

Because λ_H^* is linear on e_1 and e_2, there are nonzero constants a and b of the same sign such that

$$\lambda_H^*\big|_{e_1} = a\lambda_H\big|_{e_1} \quad\text{and}\quad \lambda_H^*\big|_{e_2} = b\lambda_H\big|_{e_2}. \tag{4.5}$$

Therefore, on the sides $e_1 \cup e_2$,

$$\begin{aligned}\lambda_H(\mathbf{x})^{r-2}\tilde{R}_V(\mathbf{x}) &\\ = \frac{a^{r-2}-b^{r-2}}{a^{r-2}+b^{r-2}}\lambda_H(\mathbf{x})^{r-2} &+ \frac{2}{a^{r-2}+b^{r-2}}(\lambda_H(\mathbf{x})^*)^{r-2}\tilde{R}_V(\mathbf{x}), \quad \mathbf{x}\in e_1\cup e_2.\end{aligned} \tag{4.6}$$

We define the sets

$$\begin{aligned}\mathcal{A}^1 &= \operatorname{span}\{1,\lambda_H,\dots,\lambda_H^{r-2},\lambda_{12},\lambda_H\lambda_{12},\dots,\lambda_H^{r-3}\lambda_{12},\lambda_H^{r-2}\tilde{R}_V\},\\ \mathcal{A}^2 &= \operatorname{span}\big\{\{1,\lambda_H,\dots,\lambda_H^{r-2}\}\otimes\{1,\tilde{R}_V\}\big\},\\ \mathcal{A}^{1,\sim} &= \operatorname{span}\{1,\lambda_H,\dots,\lambda_H^{r-2},\lambda_{12},\lambda_H\lambda_{12},\dots,\lambda_H^{r-3}\lambda_{12},(\lambda_H^*)^{r-2}\tilde{R}_V\},\\ \mathcal{A}^{1,*} &= \operatorname{span}\{1,\lambda_H,\dots,\lambda_H^{r-2},\lambda_{12},\lambda_H\lambda_{12},\dots,\lambda_H^{r-3}\lambda_{12},(\lambda_H^*)^{r-2}R_V\},\end{aligned}$$

The later set $\mathcal{A}^{1,*}$, times $F_E^0(1-\hat{x}_2^2)$, defines the shape functions for our direct serendipity finite element based on the mapped supplement (4.2). However, we can replace

R_V by $\tilde{R}_V$, since we consider only DoFs. That is, $\mathcal{A}^{1,\sim}$ and $\mathcal{A}^{1,*}$ are equivalent for our purposes. Lemma 3.1 shows that $\mathcal{A}^1 = \mathcal{A}^2$, which is unisolvent. Moreover, (4.6) shows that $\mathcal{A}^1 \subset \mathcal{A}^{1,\sim}$, which have the same dimension and so are equal, and hence we have unisolvence. Unisolvence is maintained after multiplication by $F_E^0(1-\hat{x}_2^2)$, since this modification concerns the fact that there are $c_1 > 0$ and $c_2 > 0$ so that

$$F_E^0(1-\hat{x}_2^2)\big|_{e_j} = c_j \lambda_3 \lambda_4, \quad j = 1, 2. \tag{4.7}$$

We conclude that the direct serendipity element with the mapped supplements (4.2)–(4.3), i.e.,

$$\mathcal{DS}_r^{\mathrm{map}}(E) = \mathbb{P}_r(E) \oplus \mathrm{span}\{F_E^0\big((1-\hat{x}_2^2)\hat{x}_1\hat{x}_2^{r-2}\big), F_E^0\big((1-\hat{x}_1^2)\hat{x}_2\hat{x}_1^{r-2}\big)\}, \tag{4.8}$$

is well defined.

5. The de Rham complex and mixed finite elements. The de Rham complex of interest here is

$$\mathbb{R} \hookrightarrow H^1 \xrightarrow{\mathrm{curl}} H(\mathrm{div}) \xrightarrow{\mathrm{div}} L^2 \longrightarrow 0, \tag{5.1}$$

where the curl (or rot) of a scalar function $\phi(\mathbf{x}) = \phi(x_1, x_2)$ is $\mathrm{curl}\,\phi = \left(\dfrac{\partial\phi}{\partial x_2}, -\dfrac{\partial\phi}{\partial x_1}\right)$. From right to left, the image of one linear map is the kernel of the next. On rectangular elements, it is known [4, 5] that the serendipity space $\mathcal{S}_{r+1}$ is the precursor of the Brezzi-Douglas-Marini space BDM_r [18] for $r \geq 1$; that is, on the reference square $\hat{E}$, (1.1) holds.

5.1. Full and reduced AC spaces. We have the following extension of (1.1) to quadrilateral elements E. The direct serendipity spaces $\mathcal{DS}_r^{\mathrm{map}}$ using the mapped supplements (4.2)–(4.3) is the precursor of the reduced $H(\mathrm{div})$-approximating Arbogast-Correa space $\mathrm{AC}_r^{\mathrm{red}}$ [1], $r \geq 1$, defined on meshes of convex quadrilaterals:

$$\mathbb{R} \hookrightarrow \mathcal{DS}_{r+1}^{\mathrm{map}}(E) \xrightarrow{\mathrm{curl}} \mathrm{AC}_r^{\mathrm{red}}(E) \xrightarrow{\mathrm{div}} \mathbb{P}_{r-1}(E) \longrightarrow 0. \tag{5.2}$$

Moreover, the full $H(\mathrm{div})$-approximating space AC_r, for $r \geq 1$, satisfies

$$\mathbb{R} \hookrightarrow \mathcal{DS}_{r+1}^{\mathrm{map}}(E) \xrightarrow{\mathrm{curl}} \mathrm{AC}_r(E) \xrightarrow{\mathrm{div}} \mathbb{P}_r(E) \longrightarrow 0. \tag{5.3}$$

This observation is clear once one realizes three sets of facts. First, the direct serendipity elements based on (4.2)–(4.3) have the structure

$$\mathcal{DS}_{r+1}^{\mathrm{map}}(E) = \mathbb{P}_{r+1}(E) \oplus \mathbb{S}_{r+1}^{\mathcal{DS},\mathrm{map}}(E), \tag{5.4}$$

$$\mathbb{S}_{r+1}^{\mathcal{DS},\mathrm{map}}(E) = \mathrm{span}\big\{F_E^0\big((1-\hat{x}_2^2)\hat{x}_1\hat{x}_2^{r-1}\big), F_E^0\big((1-\hat{x}_1^2)\hat{x}_2\hat{x}_1^{r-1}\big)\big\}. \tag{5.5}$$

Second, the AC elements have the structure

$$\mathrm{AC}_r(E) = \mathrm{AC}_r^{\mathrm{red}}(E) \oplus \mathbf{x}\tilde{\mathbb{P}}_r(E), \tag{5.6}$$

$$\mathrm{AC}_r^{\mathrm{red}}(E) = \mathbb{P}_r^2(E) \oplus \mathbb{S}_{r+1}^{\mathrm{AC}}(E), \tag{5.7}$$

$$\mathbb{S}_{r+1}^{\mathrm{AC}}(E) = \mathrm{span}\big\{\mathbf{F}_E^1\,\mathrm{curl}\big((1-\hat{x}_2^2)\hat{x}_1\hat{x}_2^{r-1}\big), \mathbf{F}_E^1\,\mathrm{curl}\big((1-\hat{x}_1^2)\hat{x}_2\hat{x}_1^{r-1}\big)\big\}, \tag{5.8}$$

where $\mathbf{F}_E^1$ is the Piola mapping from E to $\hat{E}$. Finally, we have the fairly well-known helmholtz-like decomposition (see, e.g., [1])

$$\mathbb{P}_r^2(E) = \mathrm{curl}\,\mathbb{P}_{r+1}^2(E) \oplus \mathbf{x}\tilde{\mathbb{P}}_{r-1}(E), \tag{5.9}$$

the relation between the curl operator and the bilinear and Piola maps

$$\operatorname{curl} F_E^0 = \mathbf{F}_E^1 \operatorname{curl}, \tag{5.10}$$

and the fact that the div operator takes $\mathbf{x}\mathbb{P}_k$ one-to-one and onto $\mathbb{P}_k$ for any $k \geq 0$.

Now we see that

$$\begin{aligned} \operatorname{curl} \mathbb{S}_{r+1}^{\mathcal{DS},\mathrm{map}}(E) &= \operatorname{span}\big\{\operatorname{curl} F_E^0\big((1-\hat{x}_2^2)\hat{x}_1\hat{x}_2^{r-1}\big), \operatorname{curl} F_E^0\big((1-\hat{x}_1^2)\hat{x}_2\hat{x}_1^{r-1}\big)\big\} \\ &= \operatorname{span}\big\{\mathbf{F}_E^1 \operatorname{curl}\big((1-\hat{x}_2^2)\hat{x}_1\hat{x}_2^{r-1}\big), \mathbf{F}_E^1 \operatorname{curl}\big((1-\hat{x}_1^2)\hat{x}_2\hat{x}_1^{r-1}\big)\big\} \\ &= \mathbb{S}_r^{\mathrm{AC}}(E), \end{aligned} \tag{5.11}$$

and so

$$\operatorname{curl} \mathcal{DS}_{r+1}^{\mathrm{map}}(E) = \operatorname{curl} \mathbb{P}_{r+1}(E) \oplus \mathbb{S}_r^{\mathrm{AC}}(E) \tag{5.12}$$

is in the kernel of the operator div. Finally,

$$\mathrm{AC}_r^{\mathrm{red}}(E) = \operatorname{curl} \mathbb{P}_{r+1}(E) \oplus \mathbb{S}_r^{\mathrm{AC}}(E) \oplus \mathbf{x}\tilde{\mathbb{P}}_{r-1}(E), \tag{5.13}$$

$$\mathrm{AC}_r(E) = \operatorname{curl} \mathbb{P}_{r+1}(E) \oplus \mathbb{S}_r^{\mathrm{AC}}(E) \oplus \mathbf{x}\tilde{\mathbb{P}}_{r}(E), \tag{5.14}$$

satisfy the properties of the de Rham complex (5.2)–(5.3).

We remark that it is easy to check that $\mathcal{S}_1(E)$ (see (3.1)) precedes the element $\mathrm{AC}_0(\mathrm{E})$ in the de Rham sequence (5.3).

5.2. Direct mixed finite elements on quadrilaterals. The de Rham theory provides a way of constructing a mixed finite element space $\mathbf{V}_r$ based on a well defined direct serendipity space. Tangential derivatives of functions in $\mathcal{DS}_{r+1}(E)$ along the edges map by the curl operator to normal derivatives; that is, if we define the unit tangential vector

$$\tau_i = (-\nu_{i,2}, \nu_{i,1}) \quad \text{on } e_i, \tag{5.15}$$

then for $\phi \in \mathcal{DS}_{r+1}(E)$,

$$\nabla\phi \cdot \tau_i\big|_{e_i} = \operatorname{curl} \phi \cdot \nu_i\big|_{e_i}. \tag{5.16}$$

Since $\operatorname{curl} \mathcal{DS}_{r+1}(E)$ spans $\mathbb{P}_r(e_i)$ independently of the other sides, the same is true of the normal derivatives of $\mathbf{V}_r(E)$. In fact, for $r \geq 1$, we have de Rham complexes for both full and reduced direct $H(\mathrm{div})$-approximating mixed elements:

$$\mathbb{R} \hookrightarrow \mathcal{DS}_{r+1}(E) \xrightarrow{\operatorname{curl}} \mathbf{V}_r^{\mathrm{full}}(E) \xrightarrow{\operatorname{div}} \mathbb{P}_r(E) \longrightarrow 0, \tag{5.17}$$

$$\mathbb{R} \hookrightarrow \mathcal{DS}_{r+1}(E) \xrightarrow{\operatorname{curl}} \mathbf{V}_r^{\mathrm{red}}(E) \xrightarrow{\operatorname{div}} \mathbb{P}_{r-1}(E) \longrightarrow 0, \tag{5.18}$$

for any variant of our new direct serendipity spaces. To see this fact, we need to decompose $\mathbf{V}_r(E)$ (i.e, $\mathbf{V}_r^{\mathrm{full}}(E)$ or $\mathbf{V}_r^{\mathrm{red}}(E)$).

According to [1], a reduced or full $H(\mathrm{div})$-approximating mixed finite element space defined directly on a quadrilateral E of minimal local dimension takes the form ($\mathcal{P}$ in Definition 2.1)

$$\mathbf{V}_r^{\mathrm{full}}(E) = \mathbb{P}_r^2(E) \oplus \mathbf{x}\tilde{\mathbb{P}}_r \oplus \mathbb{S}_r^{\mathbf{V}}(E) = \operatorname{curl} \mathbb{P}_{r+1}(E) \oplus \mathbf{x}\mathbb{P}_r \oplus \mathbb{S}_r^{\mathbf{V}}(E), \tag{5.19}$$

$$\mathbf{V}_r^{\mathrm{red}}(E) = \mathbb{P}_r^2(E) \oplus \mathbb{S}_r^{\mathbf{V}}(E) \qquad = \operatorname{curl} \mathbb{P}_{r+1}(E) \oplus \mathbf{x}\mathbb{P}_{r-1} \oplus \mathbb{S}_r^{\mathbf{V}}(E), \tag{5.20}$$

where the choice of $\mathbb{S}_r^{\mathbf{V}}(E)$ is given by taking (5.8). However, it is noted that other supplemental functions could be used [1, near (3.15)]. Their normal components must lie in $\mathbb{P}_r(e_i)$ on each edge e_i and, if they are mapped by the Piola transform, they must contain a nontrivial component of the DoFs of $\operatorname{curl} \hat{x}^{r+1}\hat{y}$ and $\operatorname{curl} \hat{x}\hat{y}^{r+1}$.

As given in [1], the DoFs ($\mathcal{N}$ in Definition 2.1) for $\boldsymbol{\psi} \in \mathbf{V}_r^{\text{full}}(E)$ $(s = r)$ or $\boldsymbol{\psi} \in \mathbf{V}_r^{\text{red}}(E)$ $(s = r-1)$ are

$$\int_{e_i} \boldsymbol{\psi} \cdot \nu_i \, p \, dx, \quad \forall p \in \mathbb{P}_r(e_i), \ i = 1,2,3,4, \tag{5.21}$$

$$\int_E \boldsymbol{\psi} \cdot \nabla q \, dx, \quad \forall q \in \mathbb{P}_s(E), \tag{5.22}$$

$$\int_E \boldsymbol{\psi} \cdot \mathbf{v} \, dx, \qquad \forall p \in \mathbb{B}_r^{\mathbf{V}}(E), \tag{5.23}$$

where the $H(\text{div})$ bubble functions are

$$\mathbb{B}_r^{\mathbf{V}}(E) = \operatorname{curl}\big(\lambda_1\lambda_2\lambda_3\lambda_4\mathbb{P}_{r-3}(E)\big). \tag{5.24}$$

The DoFs (5.22) are determined entirely by the part of $\mathbf{V}_r^{\text{full}}(E)$ or $\mathbf{V}_r^{\text{red}}(E)$ in the decomposition (5.19)–(5.20) that is $\mathbf{x}\mathbb{P}_r$ or $\mathbf{x}\mathbb{P}_{r-1}$, respectively. The DoFs (5.23) correspond to the interior cell direct serendipity DoFs. In fact, $\mathbb{B}_r^{\mathbf{V}}(E)$ is exactly the curl of the span of the cell shape functions (3.5) for $\mathcal{DS}_{r+1}(E)$. The DoFs (5.21) correspond to the edge and vertex DoFs of $\mathcal{DS}_{r+1}(E)$.

We can use any of our direct serendipity spaces to define the supplemental space $\mathbb{S}_r^{\mathbf{V}}(E)$ needed by $\mathbf{V}_r^{\text{full}}(E)$ or $\mathbf{V}_r^{\text{red}}(E)$. The rest of the space is composed of polynomials, and so need not be defined by $\mathcal{DS}_{r+1}(E)$ through the curl operator, although this strategy could be used to help construct a basis for $\mathbf{V}_r(E)$ respecting the DoFs. On E when $r \geq 1$, our new mixed spaces use the supplemental space

$$\mathbb{S}_r^{\mathbf{V}}(E) = \operatorname{curl} \mathbb{S}_{r+1}^{\mathcal{DS}}(E). \tag{5.25}$$

In particular, as we saw, $\operatorname{curl} \mathbb{S}_{r+1}^{\mathcal{DS},\text{map}}(E)$ gives the supplements for the elements $\text{AC}_r(E)$. If we use the fully direct serendipity supplements from (3.6), we obtain new families of fully direct mixed elements. The computations are not difficult. Note that

$$\operatorname{curl} \lambda_j = -\operatorname{curl}\big((\mathbf{x} - \mathbf{x}_j) \cdot \nu_j\big) = \tau_j. \tag{5.26}$$

Suppose that λ_H is represented by (4.4) (i.e., the zero line is orthogonal to ν_H) and define $\tau_H = (-\nu_{H,2}, \nu_{H,1})$, so $\operatorname{curl} \lambda_H = \tau_H$. If we use (3.12)–(3.13) to define R_V and R_H, the supplemental space is (recall (3.6))

$$\mathbb{S}_r^{\mathbf{V}}(E) = \operatorname{span}\{\boldsymbol{\sigma}_{r,1}, \boldsymbol{\sigma}_{r,2}\}, \tag{5.27}$$

$$\begin{aligned}\boldsymbol{\sigma}_{r,1} = \operatorname{curl}(R_V^{\text{simple}}\lambda_H^{r-1}\lambda_3\lambda_4) &= \lambda_H^{r-1}\lambda_3\lambda_4\frac{(\xi_V^{-1} + \eta_V^{-1})(\lambda_2\tau_1 - \lambda_1\tau_2)}{(\xi_V^{-1}\lambda_1 + \eta_V^{-1}\lambda_2)^2} \\ &+ (r-1)R_V^{\text{simple}}\lambda_H^{r-2}\lambda_3\lambda_4\tau_H + R_V^{\text{simple}}\lambda_H^{r-1}(\lambda_4\tau_3 + \lambda_3\tau_4),\end{aligned} \tag{5.28}$$

$$\begin{aligned}\boldsymbol{\sigma}_{r,2} = \operatorname{curl}(R_H^{\text{simple}}\lambda_V^{r-1}\lambda_1\lambda_2) &= \lambda_V^{r-1}\lambda_1\lambda_2\frac{(\xi_H^{-1} + \eta_H^{-1})(\lambda_4\tau_3 - \lambda_3\tau_4)}{(\xi_H^{-1}\lambda_3 + \eta_H^{-1}\lambda_4)^2} \\ &+ (r-1)R_H^{\text{simple}}\lambda_V^{r-2}\lambda_1\lambda_2\tau_V + R_H^{\text{simple}}\lambda_V^{r-1}(\lambda_2\tau_1 + \lambda_1\tau_2).\end{aligned} \tag{5.29}$$

The normal flux on each edge is easy to compute. For $\boldsymbol{\sigma}_{r,1}$, we have

$$\begin{aligned}
\boldsymbol{\sigma}_{r,1}\cdot\nu_1\big|_{e_1} &= -\eta_V\lambda_H^{r-2}\big((r-1)\lambda_3\lambda_4\tau_H\cdot\nu_1+\lambda_H\left(\lambda_4\tau_3\cdot\nu_1+\lambda_3\tau_4\cdot\nu_1\right)\big),\\
\boldsymbol{\sigma}_{r,1}\cdot\nu_2\big|_{e_2} &= \xi_V\lambda_H^{r-2}\big((r-1)\lambda_3\lambda_4\tau_H\cdot\nu_2+\lambda_H\left(\lambda_4\tau_3\cdot\nu_2+\lambda_3\tau_4\cdot\nu_2\right)\big),\\
\boldsymbol{\sigma}_{r,1}\cdot\nu_3\big|_{e_3} &= \boldsymbol{\sigma}_{r,1}\cdot\nu_4\big|_{e_4} = 0.
\end{aligned}$$

It is readily apparent that, indeed, the normal fluxes are in $\mathbb{P}_r(e_i)$ for each i.

5.3. Implementation as an $H(\mathbf{div})$-conforming mixed space. The mixed space of vector functions $\mathbf{V}_r$ over Ω is defined by merging continuously the normal fluxes across each edge e of the mesh $\mathcal{T}_h$. That is,

$$\mathbf{V}_r^{\text{full}} = \big\{\mathbf{v}\in H(\text{div};\Omega)\ :\ \mathbf{v}\big|_E\in\mathbf{V}_r^{\text{full}}(E)\text{ for all }E\in\mathcal{T}_h\big\}, \tag{5.30}$$

$$\mathbf{V}_r^{\text{red}} = \big\{\mathbf{v}\in H(\text{div};\Omega)\ :\ \mathbf{v}\big|_E\in\mathbf{V}_r^{\text{red}}(E)\text{ for all }E\in\mathcal{T}_h\big\}. \tag{5.31}$$

This can be done locally by constructing a local basis respecting the (edge) DoFs, in a way similar to that described for the serendipity elements in Section 3.5. However, in practical implementation, the hybrid form of the mixed method is often used [8]. In that case, the elements are simply concatenated and no DoF-basis is required. The Lagrange multiplier space, used to enforce the normal flux continuity, is simply

$$\Lambda_r = \big\{\lambda\in L^2\big(\cup_{E\in\mathcal{T}_h}\partial E\big)\ :\ \lambda\big|_e\in\mathbb{P}_r(e)\text{ for each edge }e\text{ of }\mathcal{T}_f\big\}. \tag{5.32}$$

The mixed space of vector functions $\mathbf{V}_r^{\text{full}}$ or $\mathbf{V}_r^{\text{red}}$ is normally paired with a space approximating scalar functions

$$W_s = \big\{w\in L^2(\Omega)\ :\ w\big|_E\in\mathbb{P}_s(E)\text{ for all }E\in\mathcal{T}_h\big\}, \tag{5.33}$$

denoted $W_r^{\text{full}}=W_r$ or $W_r^{\text{red}}=W_{r-1}$, respectively. These spaces are the divergences of the corresponding vector function spaces.

6. Stability and convergence properties. In this section, we summarize the stability and convergence theory for our new direct finite elements. For the most part, we work over the entire domain Ω.

6.1. Direct serendipity element properties. In Section 3.5, we discussed creating a local nodal basis for some of the shape functions of $\mathcal{DS}_r(E)$. By Theorem 3.2, there exists a fully nodal basis; that is, one for which every basis function vanishes at all but one nodal point. We denote it as $\{\varphi_1,\dots,\varphi_{\dim\mathcal{DS}_r(E)}\}$.

DEFINITION 6.1. *Given the r-th order direct serendipity element $(E,\mathcal{DS}_r(E),\mathcal{N})$ and the nodal basis of $\mathcal{DS}_r(E)$, $\{\varphi_1,\dots,\varphi_{\dim\mathcal{DS}_r(E)}\}$, let the operator $\mathcal{I}_E: L^2(E)\cap\mathcal{C}^0(E)\longrightarrow\mathcal{DS}_r(E)$ be interpolation. That is, for $\phi\in L^2(E)\cap\mathcal{C}^0(E)$,*

$$\mathcal{I}_E\,\phi = \sum_{j=1}^{\dim\mathcal{DS}_r(E)} N_j(\phi)\,\varphi_j = \sum_{j=1}^{\dim\mathcal{DS}_r(E)} \phi(\mathbf{x}_j)\,\varphi_j\in\mathcal{DS}_r(E).$$

Given the finite element space $\mathcal{DS}_r$ over Ω, let the operator $\mathcal{I}_h$ be global interpolation. That is, for a given function $\phi\in L^2(\Omega)\cap\mathcal{C}^0(\Omega)$, $\mathcal{I}_h\,v\in\mathcal{DS}_r$ and $\mathcal{I}_h\,\phi\big|_E=\mathcal{I}_E\,\phi$.

By Theorem 3.2, the local interpolation operator preserves polynomials, so we have an important property [20, pp. 121–123] expressed in the following lemma.

LEMMA 6.2. *The interpolation operator $\mathcal{I}_E$ is polynomial preserving, i.e., $\forall \psi \in \mathbb{P}_r(E)$, $\mathcal{I}_E\,\psi = \psi$. Moreover, $\|\mathcal{I}_E\|$ is bounded in the L^2-norm.*

With this lemma and Theorem 3.2, we have the analogue of the Bramble-Hilbert [16] or Dupont-Scott [24] lemma for local and global error estimation, provided the mesh is shape regular.

LEMMA 6.3. *There exists a constant $C > 0$ such that for all functions $\phi \in H^{s+1}(E)$ $(H^1(E) \cap \mathcal{C}^0(E)$ if $s = 0)$,*

$$|\phi - \mathcal{I}_E\,\phi|_{m,E} \leq C\, h_E^{s+1-m}\, |\phi|_{s+1,E}, \quad m = 0, 1 \text{ and } s = 0, 1, \ldots, r, \tag{6.1}$$

where $|\cdot|_{m,E}$ is the $H^m(E)$ seminorm. Moreover, suppose that $\mathcal{T}_h$ is uniformly shape regular as $h \to 0$. Then there exists a constant $C > 0$, independent of h, such that for all functions $\phi \in H^{s+1}(\Omega)$ $(\phi \in H^1(\Omega) \cap \mathcal{C}^0(\overline{\Omega})$ if $s = 0)$,

$$|\phi - \mathcal{I}_h\,\phi|_{m,\Omega} \leq C\, h^{s+1-m}\, |\phi|_{s+1,\Omega}, \quad m = 0, 1 \text{ and } s = 0, 1 \ldots, r. \tag{6.2}$$

6.2. Direct mixed finite element properties. As was done by Raviart and Thomas [35] for their mixed spaces, we can define a projection operator, usually denoted π, mapping $H(\mathrm{div}; \Omega) \cap (L^{2+\epsilon}(\Omega))^2$, $\epsilon > 0$, onto $\mathbf{V}_r$ (full or reduced) that has several important properties. The operator π is pieced together from locally defined operators π_E. Following [1], for $\mathbf{v}$, we define $\pi_E \mathbf{v}$ in terms of the DoFs (5.21)–(5.23). The operator π satisfies the commuting diagram property [21], which is to say that

$$\mathcal{P}_{W_s} \nabla \cdot \mathbf{v} = \nabla \cdot \pi \mathbf{v}, \tag{6.3}$$

where $\mathcal{P}_{W_s}$ is the L^2-orthogonal projection operator onto $W_s = \nabla \cdot \mathbf{V}_r$ and $s = r$ for full spaces and $s = r - 1$ for reduced. Since π_E is bounded in, say, H^1, we obtain the following approximation results [16, 24, 19, 20, 14, 1].

LEMMA 6.4. *Suppose that $\mathcal{T}_h$ is uniformly shape regular as $h \to 0$. Then there is a constant $C > 0$, independent of h, such that*

$$\|\mathbf{v} - \pi \mathbf{v}\|_{0,\Omega} \leq C\, \|\mathbf{v}\|_{k,\Omega}\, h^k, \qquad k = 1, \ldots, r+1, \tag{6.4}$$

$$\|\nabla \cdot (\mathbf{v} - \pi \mathbf{v})\|_{0,\Omega} \leq C\, \|\nabla \cdot \mathbf{u}\|_{k,\Omega}\, h^k, \quad k = 0, 1, \ldots, s+1, \tag{6.5}$$

$$\|p - \mathcal{P}_{W_s} p\|_{0,\Omega} \leq C\, \|p\|_{k,\Omega}\, h^k, \qquad k = 0, 1, \ldots, s+1, \tag{6.6}$$

where $s = r \geq 1$ and $s = r - 1 \geq 0$ for full and reduced $H(div)$-approximation, respectively, and $\|\cdot\|_{m,\Omega}$ is the $H^m(\Omega)$ norm. Moreover, the discrete inf-sup condition

$$\sup_{\mathbf{v}_h \in \mathbf{V}_r} \frac{(w_h, \nabla \cdot \mathbf{v}_h)}{\|\mathbf{v}_h\|_{H(\mathrm{div})}} \geq \gamma\, \|w_h\|_{0,\Omega}, \quad \forall w_h \in W_s, \tag{6.7}$$

holds for some $\gamma > 0$ independent of h.

6.3. Application to second order elliptic equations. Consider a uniformly elliptic problem with a homogeneous Dirichlet boundary condition

$$-\nabla \cdot (\mathbf{a} \nabla p) = f \quad \text{in } \Omega, \tag{6.8}$$

$$p = 0 \quad \text{on } \partial\Omega, \tag{6.9}$$

where the second order tensor $\mathbf{a}(\mathbf{x})$ is uniformly positive definite and bounded, and $f \in L^2(\Omega)$. The boundary value problem can be written in the weak form: Find $p \in H_0^1(\Omega)$ such that

$$(\mathbf{a}\nabla p, \nabla q) = (f, q), \quad \forall q \in H_0^1(\Omega), \tag{6.10}$$

where $(\cdot,\cdot)$ is the $L^2(\Omega)$ inner product. Setting

$$\mathbf{u} = -\mathbf{a}\nabla p, \tag{6.11}$$

we also have the mixed weak form: Find $\mathbf{u} \in H(\mathrm{div};\Omega)$ and $p \in L^2(\Omega)$ such that

$$(\mathbf{a}^{-1}\mathbf{u}, \mathbf{v}) - (p, \nabla\cdot\mathbf{v}) = 0, \qquad \forall \mathbf{v} \in H(\mathrm{div};\Omega), \tag{6.12}$$

$$(\nabla\cdot\mathbf{u}, w) \qquad\qquad = (f, w), \quad \forall w \in L^2(\Omega). \tag{6.13}$$

Define the global finite element space over $\mathcal{T}_h$

$$X_{0,h} = \{v_h \in \mathcal{DS}_r \ : \ v_h = 0 \text{ on } \partial\Omega\} \subset H_0^1(\Omega).$$

We then obtain the Galerkin approximation: Find $p_h \in X_{0,h}$ such that

$$(\mathbf{a}\nabla p_h, q_h) = (f, q_h), \quad \forall q_h \in X_{0,h}. \tag{6.14}$$

Combining Céa's lemma [20, 17] and the global projection estimate Lemma 6.3, we obtain an H^1-error estimate for the problem. Since Ω is a polygonal domain, $\partial\Omega$ is a Lipschitz boundary. If we assume that Ω is also convex, we have elliptic regularity of the solution [28, Theorem 4.3.1.4], and the Aubin-Nitsche duality principle [20, 17] gives an L^2-error estimate.

THEOREM 6.5. *Let Ω be a convex polygonal domain and let $\mathcal{T}_h$ be uniformly shape regular. There exists a constant $C > 0$, independent of h, such that*

$$\|p - p_h\|_{m,\Omega} \le C\, h^{s+1-m}\, |p|_{s+1,\Omega}, \quad s = 0, 1, \ldots, r, \quad m = 0, 1, \tag{6.15}$$

where p_h satisfies (6.14).

We also have the mixed full ($s = r$) and reduced ($s = r-1$) $H(\mathrm{div})$-approximation: Find $(\mathbf{u}_h, p_h) \in \mathbf{V}_r \times W_s$ such that

$$(\mathbf{a}^{-1}\mathbf{u}_h, \mathbf{v}_h) - (p_h, \nabla\cdot\mathbf{v}_h) = 0, \qquad \forall \mathbf{v}_h \in \mathbf{V}_r, \tag{6.16}$$

$$(\nabla\cdot\mathbf{u}_h, w_h) \qquad\qquad = (f, w_h), \quad \forall w_h \in W_s. \tag{6.17}$$

THEOREM 6.6. *Let Ω be a convex polygonal domain and let $\mathcal{T}_h$ be uniformly shape regular. There exists a constant $C > 0$, independent of h, such that*

$$\|\mathbf{u} - \mathbf{u}_h\| \le C\|\mathbf{u}\|_k h^k, \quad k = 1, \ldots, r+1, \tag{6.18}$$

$$\|\nabla\cdot(\mathbf{u} - \mathbf{u}_h)\| + \|p - p_h\| \le C\|\mathbf{u}\|_k h^k, \quad k = 0, 1, \ldots, s+1, \tag{6.19}$$

where $(\mathbf{u}_h, p_h)$ satisfies (6.16)–(6.17).

7. Numerical results. In this section, we consider the test problem (6.8)–(6.9) defined on the unit square $\Omega = [0,1]^2$ with the coefficient $\mathbf{a}$ being the 2×2 identity matrix, i.e., we solve the Poisson equation. The exact solution is $u(x,y) = \sin(\pi x)\sin(\pi y)$ and the source term is $f(x,y) = 2\pi^2 \sin(\pi x)\sin(\pi y)$.

Solutions are computed on three different sequences of meshes. The first sequence, $\mathcal{T}_h^1$, is a uniform mesh of n^2 square elements (two sets of parallel edges per element). The second sequence, $\mathcal{T}_h^2$, is a mesh of n^2 trapezoids of base h and one pair of parallel edges of size $0.75h$ and $1.25h$, as proposed in [6]. The third sequence, $\mathcal{T}_h^3$, is chosen so as to have no pair of edges parallel. The first 4×4 meshes for each sequence are shown in Figure 7.1. Finer meshes are constructed by repeating the same pattern over the domain. Our computer program uses the deal.II library [12].

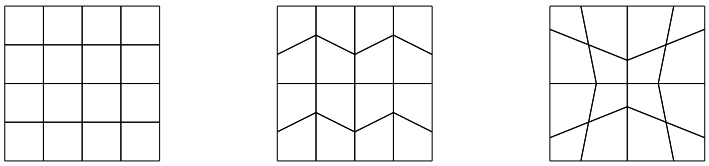

FIG. 7.1. *The three 4×4 base meshes. Finer meshes are constructed by repeating the base mesh pattern over the domain. The meshes have 2, 1, and 0 parallel edges per element, respectively.*

7.1. Fully direct serendipity spaces. In this section we present convergence studies for the fully direct serendipity spaces $\mathcal{DS}_r$ using the elements defined in (3.22). We compare the results with those of the regular serendipity spaces $\mathcal{S}_r$ and the spaces of elements given by mapping the local tensor product space $\mathbb{P}_{r,r}(\hat{E})$ to the mesh elements (hereafter simply called the $\mathbb{P}_{r,r}$ space).

As described above, one may need to consider whether opposite faces are parallel to construct a fully direct serendipity element. We now give a simple choice of element that avoids this difficulty. First, we can take (3.9) for λ_H and λ_V. Let R_V and R_H be defined by (3.12)–(3.13), where we define $\nu_H = (\nu_3 - \nu_4)/|\nu_3 - \nu_4|$ and $\nu_V = (\nu_1 - \nu_2)/|\nu_1 - \nu_2|$, and set

$$\begin{aligned} \xi_V^{-1} &= \sqrt{1 - (\nu_H \cdot \nu_1)^2}, \qquad \eta_V^{-1} = \sqrt{1 - (\nu_H \cdot \nu_3)^2}, \\ \xi_H^{-1} &= \sqrt{1 - (\nu_V \cdot \nu_2)^2}, \qquad \eta_H^{-1} = \sqrt{1 - (\nu_V \cdot \nu_4)^2}. \end{aligned} \tag{7.1}$$

For an $n \times n$ mesh, the total number of degrees of freedom for $\mathbb{P}_{r,r}$ is $(nr+1)^2 = \mathcal{O}(r^2 n^2)$, and for $\mathcal{S}_r$ and $\mathcal{DS}_r$ it is

$$\begin{aligned} \dim(\mathcal{S}_r) = \dim(\mathcal{DS}_r) &= (\text{number of vertices}) + (\text{number of edges})(r-1) \\ &\quad + (\text{number of cells})\tfrac{1}{2}(r-2)(r-3) \\ &= (n+1)^2 + 2n(n+1)(r-1) + n^2\tfrac{1}{2}(r-2)(r-3) \\ &= \tfrac{1}{2}(r^2 - r + 4)n^2 + 2rn + 1 = \mathcal{O}\left(\tfrac{1}{2}(r^2 - r + 4)n^2\right). \end{aligned}$$

Therefore, the total number of degrees of freedom for a serendipity space is asymptotically about half the size of that for a tensor product space of the same order.

We report the L^2-errors and the orders of the convergence of the spaces $\mathbb{P}_{r,r}$, $\mathcal{S}_r$ and $\mathcal{DS}_r$ for $r = 2, 3, 4, 5$ on mesh sequence $\mathcal{T}_h^1$ in Table 7.1. The errors and convergence rates in the H^1-seminorm are presented in Table 7.2. Since $\mathcal{T}_h^1$ is a sequence of square meshes, the direct serendipity space $\mathcal{DS}_r$ and the regular serendipity space $\mathcal{S}_r$ coincide on $\mathcal{T}_h^1$. All three families of spaces show an $(r+1)$-st order convergence in the L^2-norm and an r-th order convergence in the H^1-seminorm, as we should expect from theory. The errors for $\mathbb{P}_{r,r}$ are smaller than that for $\mathcal{DS}_r = \mathcal{S}_r$, but $\mathbb{P}_{r,r}$ uses many more degrees of freedom.

TABLE 7.1
L^2-errors and convergence rates for $\mathbb{P}_{r,r}$, $\mathcal{DS}_r$, and $\mathcal{S}_r$ spaces on square meshes.

	$r=2$		$r=3$		$r=4$		$r=5$	
n	error	rate	error	rate	error	rate	error	rate
$\mathbb{P}_{r,r}$ on $\mathcal{T}_h^1$ meshes								
8	2.451e-04	2.99	5.564e-06	3.99	1.054e-07	4.99	1.688e-09	6.00
12	7.282e-05	2.99	1.101e-06	4.00	1.389e-08	5.00	1.483e-10	6.00
16	3.075e-05	3.00	3.486e-07	4.00	3.298e-09	5.00	2.640e-11	6.00
24	9.116e-06	3.00	6.890e-08	4.00	4.344e-10	5.00	2.420e-12	5.89
$\mathcal{S}_r=\mathcal{DS}_r$ on $\mathcal{T}_h^1$ meshes								
8	2.457e-04	2.99	1.805e-05	4.09	1.422e-06	5.01	6.440e-08	5.93
12	7.289e-05	3.00	3.497e-06	4.05	1.870e-07	5.00	5.739e-09	5.96
16	3.076e-05	3.00	1.099e-06	4.02	4.437e-08	5.00	1.027e-09	5.98
24	9.118e-06	3.00	2.161e-07	4.01	5.841e-09	5.00	9.049e-11	5.99

TABLE 7.2
H^1-seminorm errors and convergence rates for $\mathbb{P}_{r,r}$, $\mathcal{DS}_r$, and $\mathcal{S}_r$ spaces on square meshes.

	$r=2$		$r=3$		$r=4$		$r=5$	
n	error	rate	error	rate	error	rate	error	rate
$\mathbb{P}_{r,r}$ on $\mathcal{T}_h^1$ meshes								
8	1.276e-02	2.00	4.233e-04	3.00	1.047e-05	4.00	2.066e-07	5.00
12	5.673e-03	2.00	1.255e-04	3.00	2.070e-06	4.00	2.723e-08	5.00
16	3.191e-03	2.00	5.295e-05	3.00	6.549e-07	4.00	6.462e-09	5.00
24	1.418e-03	2.00	1.569e-05	3.00	1.294e-07	4.00	8.511e-10	5.00
$\mathcal{S}_r=\mathcal{DS}_r$ on $\mathcal{T}_h^1$ meshes								
8	1.285e-02	2.02	1.537e-03	3.05	1.141e-04	3.99	5.201e-06	4.99
12	5.690e-03	2.01	4.507e-04	3.03	2.261e-05	3.99	6.856e-07	5.00
16	3.197e-03	2.00	1.894e-04	3.01	7.164e-06	4.00	1.628e-07	5.00
24	1.420e-03	2.00	5.597e-05	3.01	1.416e-06	4.00	2.144e-08	5.00

Tables 7.3–7.4 show the errors (in the L^2 and H^1-seminorms, respectively) and the orders of convergence for the trapezoidal mesh sequence $\mathcal{T}_h^2$. The tensor product space $\mathbb{P}_{r,r}$ achieves the expected optimal convergence rates. The direct serendipity space $\mathcal{DS}_r$ retains an optimal $(r+1)$-st order of convergence in the L^2 norm and an optimal r-th order convergence in the H^1-seminorm, as Theorem 6.5 predicts. The regular serendipity spaces $\mathcal{S}_r$ have worse than optimal convergence rates in both norms (as was also observed in [6]). The errors and convergence rates for $\mathbb{P}_{r,r}$, $\mathcal{DS}_r$, and $\mathcal{S}_r$ on mesh sequence $\mathcal{T}_h^3$ are similar to those on $\mathcal{T}_h^2$, so we omit showing them.

We remark that the time cost for the assembly routine can be scaled nearly perfectly in parallel, since it basically involves only local computations. Therefore, reducing the global number of degrees of freedom in a serendipity space versus a tensor product space, even perhaps at the expense of a slightly more expensive assembly, is worthwhile [40, 2].

7.2. Fully direct mixed finite elements on quadrilaterals. In this section, we verify the convergence rate for the new fully direct mixed finite elements derived in Section 5.2. These are implemented without the use of any mapping from the reference element. We take $\xi_V = \xi_H = \eta_V = \eta_H = 1$, although taking the values in

TABLE 7.3
L^2-errors and convergence rates for $\mathbb{P}_{r,r}$, $\mathcal{DS}_r$, and $\mathcal{S}_r$ spaces on trapezoidal meshes.

	$r=2$		$r=3$		$r=4$		$r=5$	
n	error	rate	error	rate	error	rate	error	rate
$\mathbb{P}_{r,r}$ on $\mathcal{T}_h^2$ meshes								
8	3.329e-04	2.99	9.740e-06	3.99	2.382e-07	4.99	5.076e-09	5.99
12	9.888e-05	2.99	1.928e-06	3.99	3.142e-08	5.00	4.462e-10	6.00
16	4.176e-05	3.00	6.107e-07	4.00	7.459e-09	5.00	7.946e-11	6.00
24	1.238e-05	3.00	1.207e-07	4.00	9.827e-10	5.00	6.979e-12	6.00
$\mathcal{S}_r$ on $\mathcal{T}_h^2$ meshes								
8	5.714e-04	2.92	4.844e-04	2.89	2.612e-05	3.72	2.005e-06	4.13
12	1.731e-04	2.94	1.482e-04	2.92	6.084e-06	3.59	3.884e-07	4.05
16	7.409e-05	2.95	6.383e-05	2.93	2.265e-06	3.43	1.234e-07	3.99
24	2.254e-05	2.94	1.963e-05	2.91	5.984e-07	3.28	2.516e-08	3.92
32	9.799e-06	2.90	8.635e-06	2.85	2.408e-07	3.16	8.342e-09	3.84
64	1.440e-06	2.70	1.332e-06	2.61	2.862e-08	3.05	6.644e-10	3.56
$\mathcal{DS}_r$ on $\mathcal{T}_h^2$ meshes								
8	3.492e-04	3.00	3.897e-05	4.07	2.187e-06	5.00	8.896e-08	5.96
12	1.036e-04	3.00	7.457e-06	4.08	2.889e-07	4.99	7.870e-09	5.98
16	4.373e-05	3.00	2.313e-06	4.07	6.868e-08	4.99	1.404e-09	5.99
24	1.296e-05	3.00	4.469e-07	4.05	9.058e-09	5.00	1.235e-10	6.00

TABLE 7.4
H^1-seminorm errors and convergence rates for $\mathbb{P}_{r,r}$, $\mathcal{DS}_r$, and $\mathcal{S}_r$ spaces on trapezoidal meshes.

	$r=2$		$r=3$		$r=4$		$r=5$	
n	error	rate	error	rate	error	rate	error	rate
$\mathbb{P}_{r,r}$ on $\mathcal{T}_h^2$ meshes								
8	1.734e-02	2.00	7.206e-04	2.99	2.310e-05	3.99	6.083e-07	4.99
12	7.710e-03	2.00	2.139e-04	3.00	4.570e-06	4.00	8.021e-08	5.00
16	4.337e-03	2.00	9.027e-05	3.00	1.447e-06	4.00	1.904e-08	5.00
24	1.928e-03	2.00	2.676e-05	3.00	2.859e-07	4.00	2.509e-09	5.00
$\mathcal{S}_r$ on $\mathcal{T}_h^2$ meshes								
8	2.413e-02	1.94	1.834e-02	1.90	1.818e-03	2.65	1.537e-04	3.18
12	1.105e-02	1.93	8.572e-03	1.88	6.582e-04	2.51	4.483e-05	3.04
16	6.432e-03	1.88	5.091e-03	1.81	3.345e-04	2.35	1.945e-05	2.90
24	3.104e-03	1.80	2.560e-03	1.70	1.360e-04	2.22	6.370e-06	2.75
32	1.920e-03	1.67	1.643e-03	1.54	7.378e-05	2.12	3.029e-06	2.58
64	7.097e-04	1.34	6.602e-04	1.23	1.776e-05	2.03	5.953e-07	2.26
$\mathcal{DS}_r$ on $\mathcal{T}_h^2$ meshes								
8	1.836e-02	2.01	2.517e-03	3.02	1.625e-04	3.99	7.384e-06	4.99
12	8.143e-03	2.00	7.400e-04	3.02	3.216e-05	4.00	9.757e-07	4.99
16	4.577e-03	2.00	3.109e-04	3.01	1.018e-05	4.00	2.318e-07	5.00
24	2.033e-03	2.00	9.170e-05	3.01	2.012e-06	4.00	3.056e-08	5.00

(7.1) provides similar results. We apply the hybrid form of the the mixed finite element method [8]. The errors and the orders of convergence for the reduced and full $H(\mathrm{div})$-

approximation spaces when $r = 1, 2$ on mesh $\mathcal{T}_h^2$ are presented in Table 7.5. Again, results are similar on $\mathcal{T}_h^3$ meshes. As the theory predicts, the scalar p, the vector $\mathbf{u}$, and the divergence $\nabla \cdot \mathbf{u}$ retain r-th, $(r+1)$-st, and r-th order approximation, respectively, for the reduced $H(\mathrm{div})$-approximation spaces, and all three quantities show r-th order approximation for the full $H(\mathrm{div})$-approximation spaces.

TABLE 7.5
Errors and convergence rates for fully direct mixed spaces on trapezoidal meshes $\mathcal{T}_h^2$.

	$\|\|p - p_h\|\|$		$\|\mathbf{u} - \mathbf{u}_h\|$		$\|\nabla \cdot (\mathbf{u} - \mathbf{u}_h)\|$	
n	error	rate	error	rate	error	rate
$r = 1$, reduced $H(\mathrm{div})$-approximation						
4	1.670e-01	—	2.609e-01	—	3.163e-00	—
8	8.271e-02	1.01	6.803e-02	1.96	1.612e-00	0.98
16	4.117e-02	1.00	1.719e-02	1.99	8.099e-01	1.00
32	2.056e-02	1.00	4.309e-03	2.00	4.054e-01	1.00
$r = 2$, reduced $H(\mathrm{div})$-approximation						
4	3.079e-02	—	2.319e-02	—	6.067e-01	—
8	7.847e-03	1.98	2.906e-03	3.00	1.549e-01	1.98
16	1.972e-03	2.00	3.633e-04	3.00	3.892e-02	2.00
32	4.936e-04	2.00	4.543e-05	3.00	9.742e-03	2.00
$r = 1$, full $H(\mathrm{div})$-approximation						
4	3.079e-02	-	5.562e-02	-	6.067e-01	-
8	7.847e-03	1.98	1.350e-02	2.02	1.549e-01	1.98
16	1.972e-03	2.00	3.355e-03	2.01	3.892e-02	2.00
32	4.936e-04	2.00	8.378e-04	2.00	9.742e-03	2.00
$r = 2$, full $H(\mathrm{div})$-approximation						
4	4.081e-03	-	7.198e-03	-	8.050e-02	-
8	5.201e-04	2.98	9.105e-04	2.99	1.026e-02	2.98
16	6.533e-05	3.00	1.141e-04	3.00	1.289e-03	3.00
32	8.176e-06	3.00	1.428e-05	3.00	1.614e-04	3.00

Our numerical test agrees with that taken in [1], where results for the full and reduced AC spaces and the mapped BDM spaces appear. Results for our fully direct mixed spaces agree very closely with the results for the AC spaces, and these far exceed the performance of the mapped BDM spaces.

7.3. Serendipity space based on mapped supplements. In this section, we present the errors and convergence rates for the serendipity spaces $\mathcal{DS}_r^{\mathrm{map}}$ using elements defined in (4.8), which has supplements mapped from the reference element. The results for $r = 2, 3, 4$ on mesh $\mathcal{T}_h^2$ are shown in Table 7.6. As predicted by the theory, this new family of spaces shows an $(r+1)$-st order convergence in the L^2-norm and an r-th order convergence in the H^1-seminorm. The results compare favorably with those for the fully direct spaces in Tables 7.3–7.4, although the latter are perhaps slightly better.

8. Summary and Conclusions. It is possible to define a wide variety of direct serendipity elements on a nondegenerate, convex quadrilateral E. Most or perhaps all of these elements appear to be new, and they have the form

$$\mathcal{DS}_r(E) = \mathbb{P}_r(E) \oplus \mathbb{S}_r^{\mathcal{DS}}(E), \quad r \geq 2. \tag{8.1}$$

TABLE 7.6
Errors and convergence rates for $\mathcal{DS}_r^{map}$ spaces on trapezoidal meshes $\mathcal{T}_h^2$.

	$r=2$		$r=3$		$r=4$		$r=5$	
n	error	rate	error	rate	error	rate	error	rate
L^2-errors and convergence rates								
8	5.737e-04	2.92	4.128e-05	4.09	2.344e-06	5.04	9.134e-08	6.00
12	1.727e-04	2.96	7.968e-06	4.06	3.048e-07	5.03	8.023e-09	6.00
16	7.329e-05	2.98	2.493e-06	4.04	7.182e-08	5.03	1.428e-09	6.00
24	2.180e-05	2.99	4.869e-07	4.03	9.380e-09	5.02	1.252e-10	6.00
H^1-seminorm errors and convergence rates								
8	2.410e-02	1.99	2.851e-03	3.05	1.730e-04	4.03	7.609e-06	5.01
12	1.074e-02	1.99	8.333e-04	3.03	3.385e-05	4.02	9.979e-07	5.01
16	6.047e-03	2.00	3.491e-04	3.02	1.065e-05	4.02	2.362e-07	5.01
24	2.690e-03	2.00	1.027e-04	3.02	2.091e-06	4.02	3.102e-08	5.01

The supplemental space $\mathbb{S}_r^{\mathcal{DS}}(E)$ can be defined by four functions. Referring to Figure 2.1, the linear functions λ_H and λ_V are arbitrary except that the zero line of λ_H must intersect the lines containing e_1 and e_2 above or below the intersection point $\mathbf{x}_{12}$, if it exists, and λ_V must intersect the lines containing e_3 and e_4 to the left or right of the intersection point $\mathbf{x}_{34}$, if it exists. The bounded, (most likely) nonlinear functions R_V and R_H can be chosen arbitrarily as long as they are negative constants on e_1 and e_3, respectively, and positive constants on e_2 and e_4, respectively. For example, one can take the simple choices

$$\lambda_H = \lambda_3 - \lambda_4, \quad R_V = \frac{\lambda_1 - \lambda_2}{\lambda_1 + \lambda_2}, \quad \lambda_V = \lambda_1 - \lambda_2, \quad R_H = \frac{\lambda_3 - \lambda_4}{\lambda_3 + \lambda_4}, \tag{8.2}$$

or the choices given in Lemma 3.1, in which case the explicit basis (3.31)–(3.35) can be constructed easily. The fully direct supplemental space is

$$\mathbb{S}_r^{\mathcal{DS}}(E) = \operatorname{span}\{\lambda_3\lambda_4\lambda_H^{r-2}R_V, \lambda_1\lambda_2\lambda_V^{r-2}R_H\}, \tag{8.3}$$

but a supplemental space can also be defined using the bilinear map between $\hat{E} = [-1,1]^2$ and E as

$$\mathbb{S}_r^{\mathcal{DS},\text{map}}(E) = \operatorname{span}\big\{F_E^0\big((1-\hat{x}_2^2)\hat{x}_1\hat{x}_2^{r-2}\big), F_E^0\big((1-\hat{x}_1^2)\hat{x}_2\hat{x}_1^{r-2}\big)\big\}. \tag{8.4}$$

It is possible to define a wide variety of direct mixed elements on E. The de Rham theory is useful in this regard, and the elements take the form

$$\mathbf{V}_r^{\text{red}}(E) = \operatorname{curl}\mathcal{DS}_{r+1}(E) \oplus \mathbf{x}\mathbb{P}_{r-1}(E) = \mathbb{P}_r^2(E) \oplus \mathbb{S}_r^{\mathbf{V}}(E) \quad r \geq 1, \tag{8.5}$$

$$\mathbf{V}_r^{\text{full}}(E) = \mathbf{V}_r^{\text{red}}(E) \oplus \mathbf{x}\tilde{\mathbb{P}}_r(E), \quad r \geq 1, \tag{8.6}$$

for reduced and full $H(\text{div})$-approximation spaces, where

$$\mathbb{S}_r^{\mathbf{V}}(E) = \operatorname{curl}\mathbb{S}_r^{\mathcal{DS}}(E). \tag{8.7}$$

If (8.4) is used, the AC spaces [1] result. Otherwise, the elements appear to be new, and they are the first families of fully direct mixed spaces defined on quadrilaterals.

The direct serendipity and mixed elements can be merged to create $H^1(\Omega)$ and $H(\text{div};\Omega)$ conforming spaces, respectively, on a mesh $\mathcal{T}_h$ of nondegenerate, convex

quadrilaterals. If the meshes are shape regular as $h \to 0$, the spaces have both optimal approximation properties and minimal local dimension. Numerical results were presented to illustrate their performance.

We close with a simple observation. Another well-known de Rham complex is

$$\mathbb{R} \hookrightarrow H^1 \xrightarrow{\text{grad}} H(\text{curl}) \xrightarrow{\text{curl}} L^2 \longrightarrow 0, \tag{8.8}$$

where the curl of a vector function $\boldsymbol{\psi} = \big(\psi_1, \psi_2\big)$ is the scalar $\operatorname{curl}\boldsymbol{\psi}(\mathbf{x}) = \dfrac{\partial \psi_1}{\partial x_2} - \dfrac{\partial \psi_2}{\partial x_1}$. This complex is essentially just a rotation of (5.1). It gives us full ($s = r$) and reduced ($s = r - 1$) direct $H(\text{curl})$-approximating elements

$$\mathbf{V}_{r,\text{curl}}(E) = \nabla\, \mathcal{DS}_{r+1}(E) \oplus (x_2, -x_1)\mathbb{P}_s. \tag{8.9}$$

These then satisfy the de Rham complexes

$$\mathbb{R} \hookrightarrow \mathcal{DS}_{r+1}(E) \xrightarrow{\text{grad}} \mathbf{V}^{\text{full}}_{r,\text{curl}}(E) \xrightarrow{\text{curl}} \mathbb{P}_r(E) \longrightarrow 0, \tag{8.10}$$

$$\mathbb{R} \hookrightarrow \mathcal{DS}_{r+1}(E) \xrightarrow{\text{grad}} \mathbf{V}^{\text{red}}_{r,\text{curl}}(E) \xrightarrow{\text{curl}} \mathbb{P}_{r-1}(E) \longrightarrow 0, \tag{8.11}$$

for any variant of our new direct serendipity spaces. We can merge these elements globally, since tangential derivatives of ϕ, say, map to tangential components of $\nabla\phi$, which are both $\nabla\phi \cdot \tau$. So we have full and reduced direct $H(\text{curl})$-approximating spaces over meshes of quadrilaterals.

REFERENCES

[1] T. Arbogast and M. R. Correa, *Two families of H(div) mixed finite elements on quadrilaterals of minimal dimension*, SIAM J. Numer. Anal., 54 (2016), pp. 3332–3356. DOI 10.1137/15M1013705.

[2] T. Arbogast and Z. Tao, *Direct serendipity finite elements on convex quadrilaterals*, Tech. Rep. ICES REPORT 17-28, Institute for Computational Engineering and Sciences, Univ. of Texas at Austin, October 2017.

[3] D. N. Arnold, *Spaces of finite element differential forms*, in Analysis and numerics of partial differential equations, Springer, 2013, pp. 117–140.

[4] D. N. Arnold and G. Awanou, *The serendipity family of finite elements*, Foundations of Computational Mathematics, 11 (2011), pp. 337–344.

[5] ———, *Finite element differential forms on cubical meshes*, Math. Comp., 83 (2014), pp. 1551–1570.

[6] D. N. Arnold, D. Boffi, and R. S. Falk, *Approximation by quadrilateral finite elements*, Math. Comp., 71 (2002), pp. 909–922.

[7] ———, *Quadrilateral H(div) finite elements*, SIAM. J. Numer. Anal., 42 (2005), pp. 2429–2451.

[8] D. N. Arnold and F. Brezzi, *Mixed and nonconforming finite element methods: Implementation, postprocessing and error estimates*, RAIRO Modél. Math. Anal. Numér., 19 (1985), pp. 7–32.

[9] D. N. Arnold, R. S. Falk, and R. Winther, *Finite element exterior calculus, homological techniques, and applications*, Acta numerica, 15 (2006), pp. 1–155.

[10] D. N. Arnold, R. S. Falk, and R. Winther, *Finite element exterior calculus: from Hodge theory to numerical stability*, Bull. Amer. Math. Soc. (N.S.), 47 (2010), pp. 281–354.

[11] D. N. Arnold and A. Logg, *Periodic table of the finite elements*, SIAM News, 47 (2014).

[12] W. Bangerth, D. Davydov, T. Heister, L. Heltai, G. Kanschat, M. Kronbichler, M. Maier, B. Turcksin, and D. Wells, *The `deal.II` library, version 8.4*, J. Numerical Math., 24 (2016), pp. 135–141.

[13] P. B. Bochev and D. Ridzal, *Rehabilitation of the lowest-order Raviart–Thomas element on quadrilateral grids*, SIAM J. Numer. Anal., 47 (2008), pp. 487–507.

[14] D. Boffi, F. Brezzi, and M. Fortin, *Mixed finite element methods and applications*, no. 44 in Springer Series in Computational Mathematics, Springer, Heidelberg, 2013.

[15] D. Boffi, F. Kikuchi, and J. Schöberl, *Edge element computation of Maxwell's eigenvalues on general quadrilateral meshes*, Mathematical Models and Methods in Applied Sciences (M3AS), 16 (2006), pp. 265–273.
[16] J. H. Bramble and S. R. Hilbert, *Estimation of linear functionals on Sobolev spaces with applications to Fourier transforms and spline interpolation*, SIAM J. Numer. Anal., 7 (1970), pp. 112–124.
[17] S. C. Brenner and L. R. Scott, *The Mathematical Theory of Finite Element Methods*, Springer-Verlag, New York, 1994.
[18] F. Brezzi, J. Douglas, Jr., and L. D. Marini, *Two families of mixed elements for second order elliptic problems*, Numer. Math., 47 (1985), pp. 217–235.
[19] F. Brezzi and M. Fortin, *Mixed and hybrid finite element methods*, Springer-Verlag, New York, 1991.
[20] P. G. Ciarlet, *The Finite Element Method for Elliptic Problems*, North-Holland, Amsterdam, 1978.
[21] J. Douglas, Jr. and J. E. Roberts, *Global estimates for mixed methods for second order elliptic equations*, Math. Comp., 44 (1985), pp. 39–52.
[22] H.-Y. Duan and G.-P. Liang, *Nonconforming elements in least-squares mixed finite element methods*, Math. Comp., 73 (2004), pp. 1–18.
[23] T. Dupont, J. Hoffman, C. Johnson, R. C. Kirby, M. G. Larson, A. Logg, and L. R. Scott, *The fenics project*, Tech. Rep. 2003–21, Chalmers Finite Element Center, Chalmers University of Technology, Goteborg, Sweden, 2003.
[24] T. Dupont and L. R. Scott, *Polynomial approximation of functions in Sobolev space*, Math. Comp., 34 (1980), pp. 441–463.
[25] M. S. Floater and M.-J. Lai, *Polygonal spline spaces and the numerical solution of the poisson equation*, SIAM J. Numer. Anal., 54 (2016), pp. 797–824.
[26] A. Gillette and T. Kloefkorn, *Trimmed serendipity finite element differential forms*, Math. Comp., (2018).
[27] V. Girault and P. A. Raviart, *Finite Element Methods for Navier-Stokes Equations: Theory and Algorithms*, Springer-Verlag, Berlin, 1986.
[28] P. Grisvard, *Elliptic Problems in Nonsmooth Domains*, Pitman, Boston, 1985.
[29] I. Hibbitt, Karlsson & Sorensen, *ABAQUS/Standard User's Manual*, 2001.
[30] V. N. Kaliakin, *Introduction to approximate solution techniques, numerical modeling, and finite element methods*, CRC Press, 2001.
[31] D. Y. Kwak and H. C. Pyo, *Mixed finite element methods for general quadrilateral grids*, Applied Mathematics and Computation, 217 (2011), pp. 6556–6565.
[32] N.-S. Lee and K.-J. Bathe, *Effects of element distortions on the performance of isoparametric elements*, Intl. J. Numer. Meth. Engineering, 36 (1993), pp. 3553–3576.
[33] J. C. Nédélec, *Mixed finite elements in* $\mathbf{R}^3$, Numer. Math., 35 (1980), pp. 315–341.
[34] A. Rand, A. Gillette, and C. Bajaj, *Quadratic serendipity finite elements on polygons using generalized barycentric coordinates*, Math. Comp., 83 (2014), pp. 2691–2716.
[35] R. A. Raviart and J. M. Thomas, *A mixed finite element method for 2nd order elliptic problems*, in Mathematical Aspects of Finite Element Methods, I. Galligani and E. Magenes, eds., no. 606 in Lecture Notes in Math., Springer-Verlag, New York, 1977, pp. 292–315.
[36] J. Shen, *Mixed Finite Element Methods: Analysis and Computational Aspects*, PhD thesis, University of Wyoming, 1992.
[37] ———, *Mixed finite element methods on distorted rectangular grids*, Tech. Rep. ISC-94-13-MATH, Institute for Scientific Computation, Texas A&M University, College Station, Texas, 1994.
[38] D. Siqueira, P. R. B. Devloo, and S. M. Gomes, *A new procedure for the construction of hierarchical high order hdiv and hcurl finite element spaces*, J. Computational and App. Math., 240 (2013), pp. 204–214.
[39] G. Strang and G. J. Fix, *An analysis of the finite element method*, Series in Automatic Computation, Prentice-Hall, Englewood Cliffs, New Jersey, 1973.
[40] Z. Tao, *Numerical Analysis of Multiphase flows in Porous Media on Non-Rectangular Geometry*, PhD thesis, University of Texas at Austin, December 2017.
[41] J. M. Thomas, *Sur l'analyse numerique des methodes d'elements finis hybrides et mixtes*, PhD thesis, Sciences Mathematiques, à l'Universite Pierre et Marie Curie, 1977.